



**Field Research Center  
Oak Ridge, Tennessee**

## **The Oak Ridge Field Research Center Conceptual Model**

D.B. Watson<sup>1</sup>, J.E. Kostka<sup>2</sup>, M.W. Fields<sup>3</sup>, P.M. Jardine<sup>1</sup>

<sup>1</sup>Environmental Sciences Division, Oak Ridge National Laboratory

<sup>2</sup>Department of Oceanography, Florida State University

<sup>3</sup>Department of Microbiology, Miami University (Ohio)

August 2004

## **1 INTRODUCTION**

The following text describes the current conceptual framework of coupled hydrological, geochemical, and microbial processes that control the fate and transport of contaminants at the Natural and Accelerated Bioremediation Research (NABIR) Field Research Center (FRC) located on the Oak Ridge Reservation. The purpose of this document is to provide investigators from various programs (e.g. NABIR, EMSP, GTL) with state of the art knowledge of subsurface processes that are operational at the FRC background and contaminated sites in an effort to support their research mission.

The text is structured to discuss the FRC background area, the overall contaminated area, and each of the five contaminated field areas (i.e. Areas 1 through 5) with emphasis on field-scale hydrology, geochemistry, and microbiology. As field research progresses over the years, coupled processes controlling contaminant immobilization or remobilization will be added to this document.

The text is a living document that will be updated as additional relevant information is obtained. Suggestions for enhancing the current conceptual framework of the Oak Ridge FRC are encouraged. Such information should be sent to Philip Jardine or David Watson of the Oak Ridge National Laboratory (jardinepm@ornl.gov, watsondb@ornl.gov, respectively)

## 2 OAK RIDGE FRC BACKGROUND AREA

This section summarizes the characteristics of the FRC background area. Select chemical, physical, and microbial properties of the background site can be found in Table 1. The background area consists of approximately 163 hectares located in West Bear Creek Valley, about 2 km from the contaminated area (Fig. 1). The area lies directly along geologic strike of the contaminated area and is, therefore, underlain by nearly identical geology, mineralogy, and structure. No known contaminants have been disposed at this location throughout the history of DOE operations. The majority of the area is heavily wooded, with the exception of the Bear Creek floodplain. Several perennial and ephemeral crosscutting streams run through the area and feed into Bear Creek.

Dozens of single and paired wells have been installed within the past 14 years throughout the background area. In addition, two heavily-instrumented experimental field sites are located within the boundaries of the area, providing an existing resource for intensive hydrologic testing and transport studies in the clastic formations. These field facilities are heavily instrumented and extremely well characterized with regard to fate and transport processes.

### Geology

#### *Bedrock and soil features*

The background area is underlain by rocks of the Cambrian Conasauga Group (Hatcher et al. 1992), including the Dismal Gap Formation (formerly Maryville Limestone) and the overlying Nolichucky Shale (Fig. 1). Both are interbedded shales, siltstones, and limestones that have undergone post-depositional deformation and dip at 45° to the south. The Maynardville Limestone underlies the southern portion of the area near Bear Creek. Although some of the discussion that follows is relevant to the Maynardville Limestone, most of the information pertaining to the background area was obtained from the two experimental field sites that are instrumented in the clastic Nolichucky Shale and Dismal Gap formations.

The bedrock beneath the experimental field sites weathers into an unconsolidated clay-rich saprolite that retains the original fractures and bedding structures (Fig. 2). Depth to competent bedrock is between 5 and 10 m based on continuous coring (Schreiber et al. 1999) and depth to auger refusal (Lee et al. 1992), and appears to be variable based on the weathering characteristics of the underlying rocks. In general, the shales tend to be fissile while the carbonate interlayers are more resistant, imparting a "washboard" shape to the saprolite/bedrock interface. The saprolite is overlain by a thin veneer of organic- and clay-rich soil with a thickness of 0.5 to 3 m that approximates the depth of the root zone. The soil layer thickens in undisturbed, wooded areas particularly in subwatershed swale regions.

Table 1. Data summaries for the FRC background area

**Water/Moisture Storage**

| <b>Saprolite</b>                     |      |  |   |  |
|--------------------------------------|------|--|---|--|
| Specific Yield                       | Sed. | 0.03 - 0.05                                | Solomon et al. 1992   | Stormflow (root) zone  |
| Storativity                          | Sed. | 0.0004 - 0.005                             | Gierke et al. 1988  | Pump test analysis; Theis & Chow methods   |
| Water Content                        | Sed. | 0.3 - 0.5 cm <sup>3</sup> /cm <sup>3</sup> | Jardine et al. 1988<br>Jardine et al. 1993a<br>Jardine et al. 1993b<br>Wilson et al. 1992<br>Wilson et al. 1993 | Large, undisturbed columns<br>Moisture retention functions                           |
| <b>Nolichucky/Dismal Gap Bedrock</b> |      |  |   |  |
| Specific Yield                       | Sed. | 0.0025 - 0.0033                            | Solomon et al. 1992   | Value is 3-10 times less than total porosity and approx. equal to fracture porosity. |
| Storativity                          | Sed. | 0.0009 - 0.002                             | Gierke et al. 1988  | Pump test analysis; Theis & Chow methods   |
| Water Content                        | Sed. | 0.1 - 0.2 cm <sup>3</sup> /cm <sup>3</sup> | Dorsch et al. 1996  | Helium porosimetry, immersion-saturation   |

**Water Quality**

| <b>Saprolite</b>        |    |               |                |  |
|-------------------------|----|---------------|----------------|--|
| Ca (mg/L)               | GW | 26 - 73       | Schreiber 1995 |  |
| Fe (mg/L)               | GW | < 0.05 - 0.90 | Schreiber 1995 |  |
| Mg (mg/L)               | GW | 1.7 - 9.4     | Schreiber 1995 |  |
| K (mg/L)                | GW | < 2.0 - 3.8   | Schreiber 1995 |  |
| Na (mg/L)               | GW | 2.7 - 120     | Schreiber 1995 |  |
| HCO <sub>3</sub> (mg/L) | GW | 98 - 330      | Schreiber 1995 |  |

|                                      |    |              |                      |                               |
|--------------------------------------|----|--------------|----------------------|-------------------------------|
| Br (mg/L)                            | GW | < 0.1 - *4.7 | Schreiber 1995       | *residual from Br tracer test |
| Cl (mg/L)                            | GW | 0.9 - 5.5    | Schreiber 1995       |                               |
| F (mg/L)                             | GW | < 0.1 - 0.37 | Schreiber 1995       |                               |
| SO <sub>4</sub> (mg/L)               | GW | 6.6 - 170    | Schreiber 1995       |                               |
| PO <sub>4</sub> (mg/L)               | GW | < 0.5        | Schreiber 1995       |                               |
| NO <sub>3</sub> (mg/L)               | GW | < 0.1 - 2.1  | Schreiber 1995       |                               |
| Org. carbon (mg/L)                   | GW | 0.25 - 3.54  | Schreiber 1995       |                               |
| Inorg. carbon (mg/L)                 | GW | 98 - 330     | Schreiber 1995       |                               |
| Turbidity (mg/L)                     | GW | 16 - 330     | Schreiber 1995       |                               |
| Alk. (mg/kg as CaCO <sub>3</sub> )   | GW | 80 - 270     | Schreiber 1995       |                               |
| pH                                   | GW | 6.9 - 8.1    | Schreiber 1995       |                               |
| Temperature (deg C)                  | GW | 4.9 - 28.4   | Schreiber 1995       |                               |
| Eh (mV)                              | GW | 550          | Jardine et al. 1993b |                               |
| TDS (mg/L)                           | GW | 152 - 714    | Schreiber 1995       |                               |
| <b>Nolichucky/Dismal Gap Bedrock</b> |    |              |                      |                               |
| Ca (mg/L)                            | GW | 7 - 67       | Schreiber 1995       |                               |
| Fe (mg/L)                            | GW | < 0.05 - 1.5 | Schreiber 1995       |                               |
| Mg (mg/L)                            | GW | 3.8 - 9.6    | Schreiber 1995       |                               |
| K (mg/L)                             | GW | < 2.0 - 3.8  | Schreiber 1995       |                               |
| Na (mg/L)                            | GW | 9.1 - 86     | Schreiber 1995       |                               |
| HCO <sub>3</sub> (mg/L)              | GW | 146 - 275    | Schreiber 1995       |                               |

|   |    |                           |                     |                               |
|---|----|---------------------------|---------------------|-------------------------------|
| Br (mg/L)   | GW | < 0.1 - *0.42             | Schreiber 1995      | *residual from Br tracer test |
| Cl (mg/L)   | GW | 0.8 - 3.7                 | Schreiber 1995      |                               |
| F (mg/L)  | GW | < 0.1 - 0.57              | Schreiber 1995      |                               |
| SO <sub>4</sub> (mg/L)  | GW | 6.4 - 110                 | Schreiber 1995      |                               |
| PO <sub>4</sub> (mg/L)  | GW | < 0.5                     | Schreiber 1995      |                               |
| NO <sub>3</sub> (mg/L)  | GW | < 0.1 - 2.2               | Schreiber 1995      |                               |
| Org. carbon (mg/L)  | GW | 0.29 - 4.68               | Schreiber 1995      |                               |
| Inorg. carbon (mg/L)  | GW | 146 - 275                 | Schreiber 1995      |                               |
| Turbidity (mg/L)  | GW | 7 - 520                   | Schreiber 1995      |                               |
| Alk. (mg/kg as CaCO <sub>3</sub> )                                | GW | 120 - 226                 | Schreiber 1995      |                               |
| pH  | GW | 7.0 - 8.5                 | Schreiber 1995      |                               |
| Temperature (deg C)   | GW | 5.7 - 28.5                | Schreiber 1995      |                               |
| DO (mg/L)   | GW | 0.02 - 4                  | From WAG 5 studies. | (located at ORNL not BCV)     |
| Fe(II)/Fe(III) (mg/L)   | GW | 0.2 - 11 / 0.2 - 14       | From WAG 5 studies. | (located at ORNL not BCV)     |
| NO <sub>2</sub> <sup>-</sup> /NO <sub>3</sub> <sup>-</sup> (mg/L) | GW | 0.003 - 0.008 / 1.3 - 4.0 | From WAG 5 studies. | (located at ORNL not BCV)     |
| S <sup>2-</sup> (mg/L)  | GW | 0.005 - 0.35              | From WAG 5 studies. | (located at ORNL not BCV)     |
| TDS (mg/L)  | GW | 214 - 530                 | Schreiber 1995      |                               |

### Transport Properties

| Saprolite                         |      |            |   |  |
|-----------------------------------|------|------------|---|--|
| Groundwater transport rates (m/d) | GW   | 0.5 - 500  | Wilson et al. 1989<br>Wilson et al. 1992<br>Wilson et al. 1993                            | Field and undisturbed column experiments   |
| Contaminant transport rates (m/d) | GW   | 0.5 - 500  | Wilson et al. 1993<br>Jardine et al. 1988<br>Jardine et al. 1993a<br>Jardine et al. 1993b | Field and undisturbed column experiments   |
| Dispersivity (cm)                 | Sed. | 8 - 27     | Gwo et al. 1995<br>Gwo et al. 1999  | Estimated from modeled tracer field experiment using multi-region numerical approach |
| Nolichucky/Dismal Gap Bedrock     |      |            |   |  |
| Groundwater transport rates (m/d) | GW   | 0.3 - 1.5  | Jardine et al. 1999   | Specific discharge via point dilution tests  |
|                                   | GW   | 100        | Jardine et al. 1999   | Mean porewater velocity  |
| Contaminant transport rates (m/d) | GW   | 0.13 - 1.0 | Jardine et al. 1999   | Specific discharge via point dilution tests  |
| Dispersivity                      | GW   | 0.1        | Jardine et al. 1999   |  |

### Permeability

| Saprolite                          |      |   |                        |   |
|------------------------------------|------|---|------------------------|---|
| Unsat. hydraulic conduct. (m/s)    | Sed. | $0.2 - 2.5 \times 10^{-5}$                | Wilson & Luxmoore 1988 | Tension infiltrometer; geometric mean; n = 39 obs.; field meas.; psi = 0, 2, 5 14 cm. |
| Sat. hydraulic conductivity (m/s)  | Sed. | $1 \times 10^{-4}$                        | Wilson & Luxmoore 1988 | Tension infiltrometer; geometric mean; n = 39 obs.; field meas.; psi = 0, 2, 5 14 cm. |
| Transmissivity (m <sup>2</sup> /s) | Sed. | $1.1 \times 10^{-4} - 6.1 \times 10^{-3}$ | Gierke et al. 1988     | Pump test analysis; Theis & Neuman methods  |

| <b>Nolichucky/Dismal Gap Bedrock</b> |      |   |                     |  |
|--------------------------------------|------|---|---------------------|--|
| Sat. hydraulic conductivity (m/s)    | Sed. | $10^{-6}$ - $10^{-11}$                      | Moore 1989          |  |
| Transmissivity (m <sup>2</sup> /s)   | Sed. | 0.58  | Solomon et al. 1992 | Geometric mean                             |
|                                      |      | $1.1 \times 10^{-4}$ - $6.1 \times 10^{-3}$ | Gierke et al. 1988  | Pump test analysis; Theis & Neuman methods |

### Solid Characteristics

| <b>Saprolite</b>                          |      |  |   |  |
|---|------|--|---|--|
| Grain size (wt % sand-silt-clay)          | Sed. | (30.8 - 50.4 - 18.8)   | Jardine et al. 1988<br>Jardine et al. 1993a<br>Jardine et al. 1993b | Exerts little control in a structured medium   |
| Bulk density (g/cm <sup>3</sup> )         | Sed. | 1.2 - 1.7  | Jardine et al. 1988<br>Jardine et al. 1993a<br>Jardine et al. 1993b | Large undisturbed columns  |
|   |      | 1.4 - 1.7  | Howard 1997   | Paraffin clod method   |
| Porosity                                  | Sed. | 0.35 - 0.49  | Howard 1997   | Paraffin clod method   |
| Mineralogy                                | Sed. | I <sub>45</sub> IS <sub>20</sub> V <sub>10</sub> K <sub>9</sub> VC <sub>6</sub> M <sub>5</sub> Q <sub>3</sub> F <sub>1</sub> | Jardine et al. 1989<br>Kooner et al. 1995                           | I: illite<br>IS: interstratified 2:1<br>V: vermiculite<br>K: kaolinite<br>VC: chloritized vermiculite<br>M: montmorillinite<br>Q: quartz<br>F: feldspar;<br>subscripts refer to wt.%<br>K quantified by DSC. |
| Cation exch. cap. (meq/g)                 | Sed. | 0.07 - 0.16  | Jardine et al. 1993a  |  |
| Reactive surface area (m <sup>2</sup> /g) | Sed. | 40   | Kooner et al. 1995  |  |
| Redox characteristics of surface (g/kg)   | Sed. | 0.4 g/kg Mn as MnO <sub>2</sub><br>26 g/kg Fe as Fe(OH) <sub>3</sub>   | See Jardine et al. 1993b for contaminant redox                      |  |



|                                   |      |   |   |   |
|-----------------------------------|------|---|---|---|
|                                   |      |   | reactions in these soils.   |   |
| Reactive chem. vs bulk chem.      | Sed. | y = 0 (sat) 50% excl.<br>y = -10 cm 0% excl.                        | Jardine et al. 1988<br>Jardine et al. 1993a<br>Jardine et al. 1993b | Water-content dependent<br>Comparing batch and column |
| Fracture and matrix structure     | Sed. | 100-200 fractures / m<br>fracture aperture 0.05-0.5 mm              | Moline et al.   | CT imaging and direct on undisturbed column           |
| <b>Nolichucky/Dismal Gap</b>      |      |   |   |   |
| Grain size (wt % sand-silt-clay)  | Sed. | N/A   |   |   |
| Bulk density (g/cm <sup>3</sup> ) | Sed. | 2.7 - 2.8   | Dorsch et al. 1996  |   |
| Porosity                          | Sed. | 10 - 20   | Dorsch et al. 1996  |   |
| Mineralogy                        | Sed. | Illites, quartz, calcite, biotite, feldspar, kaolinite, chlorite    | Schreiber 1995<br>Lee et al. 1991                                   |   |
| Cation exch. cap. (meq/g)         | Sed. | 0.001 - 0.01  | Jardine et al. 1999   |   |
| Redox characteristics of surface  | Sed. | Catalyze oxidation of Co(II) EDTA to Co(III) EDTA in presence of DO | Jardine, unpublished  |   |
| Fracture and matrix structure     | Sed. | 50 fractures / m<br>fracture aperture 0.1 mm                        | Jardine et al. 1999   |   |

### Groundwater Recharge and Discharge

|                      |  |       |                   |                                      |
|----------------------|--|-------|-------------------|--------------------------------------|
| Rainfall (cm/y)      |  | 133   | Dole et. al. 1999 | Mean for 1954-1983                   |
| Recharge rate (cm/y) |  | 20-49 | Dole et. al. 1999 | Recharge to shallow groundwater zone |
| Discharge rate (m/s) |  |       |                   |                                      |

|                                |      |   |                        |   |
|--------------------------------|------|---|------------------------|---|
| Infiltration rate (m/s)        | Sed. | $1.4 \times 10^{-4} - 5.1 \times 10^{-6}$       | Watson & Luxmoore 1986 | Tension infiltrometer; geometric mean; n = 30 obs.; field meas.; psi = 0, 2, 5 14 cm. |
| Evapotranspiration rate (cm/y) |      | 65  | Luxmoore, unpublished  |   |
| Gradient across site (m/m)     | GW   | 0.015 - 0.075 (horiz.)<br>0.005 - 0.063 (vert.) | Schreiber et al. 1998  | Range at one location; values may exceed this range, especially near streams          |

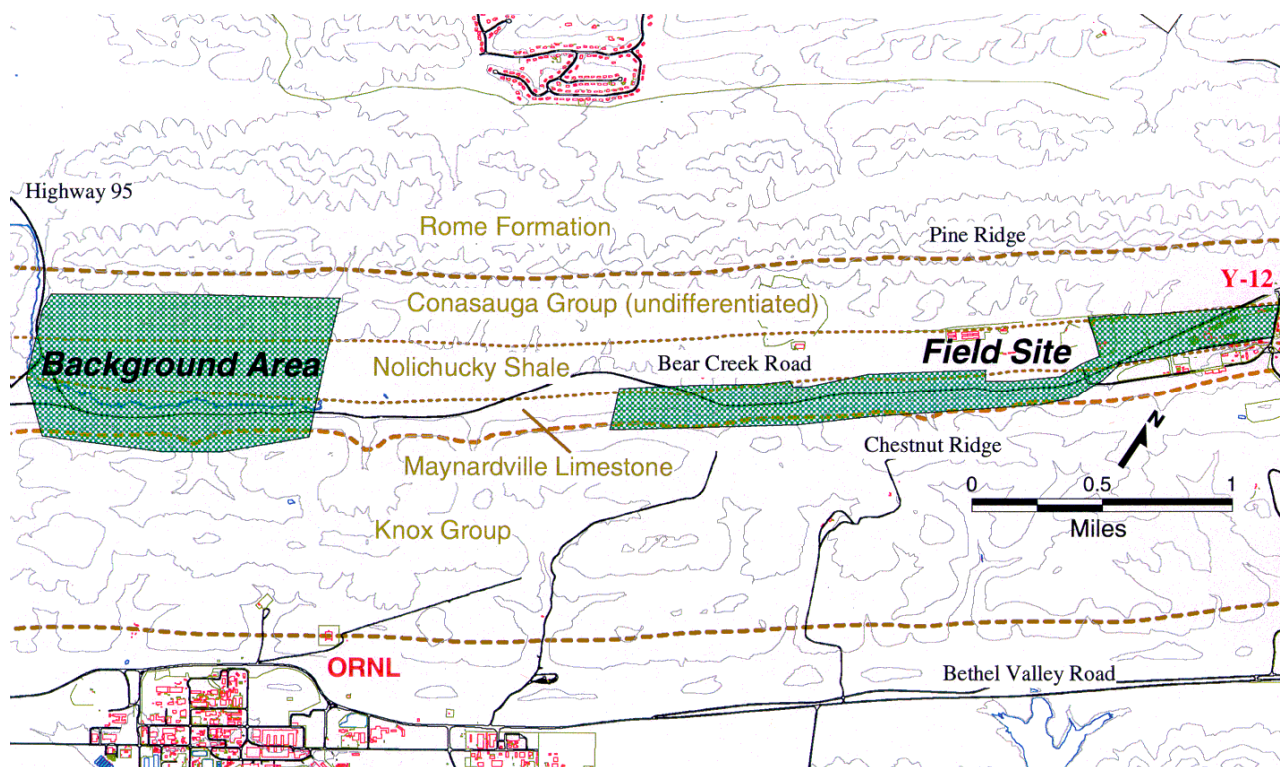


Figure 1. Location map showing FRC contaminated field sites and background area located on the same geologic units along geologic strike.

## ORNL media consisting of interbedded fractured weathered shales and limestone

---



Figure 2. Photograph of a typical saprolite soil profile and underlying interbedded shale-limestone bedrock that is present on the Oak Ridge Reservation. The more rapidly weathered limestone results in the reddish, Fe-oxide rich clay lenses present in the saprolite. The more weather resistant shales maintain relic features of the parent material and are highly fractured with a low permeability matrix.

### *Fracture characteristics*

The saprolites are acidic Inceptisols that have weathered from interbedded shale-limestone sequences. The limestone has been weathered to massive clay lenses devoid of carbonate, and the more resistant shale has weathered to an extensively fractured saprolite. Fractures are highly interconnected with densities in the range of 200 fractures/m (Dreier et.al., 1987). Fold related fractures in the saprolite are observable in the field and consist of (a) fractures along bedding planes, (b) 2 sets of orthogonal extensional fractures that are perpendicular to bedding planes, and (c) shear fractures (Fig. 3). The extensional fractures are either parallel or perpendicular to the strike of the bedding planes, and form an orthogonal fracture network with the bedding plane fractures. Bedding plane fractures dominate the fracture network of the media and have aperture spacing of  $<0.05$  mm. Cross-cutting extensional fractures are less numerous but have larger apertures ranging from 0.2-0.5 mm. Many of the fracture surfaces contain secondary deposits (e.g. clays, Mn- and Fe-oxides) suggesting that they are hydrologically active. Fracture orientation and

connectivity can give rise to extensive preferential flow within the media (Solomon et al., 1992; Wilson et al., 1993; Jardine et al., 2001).

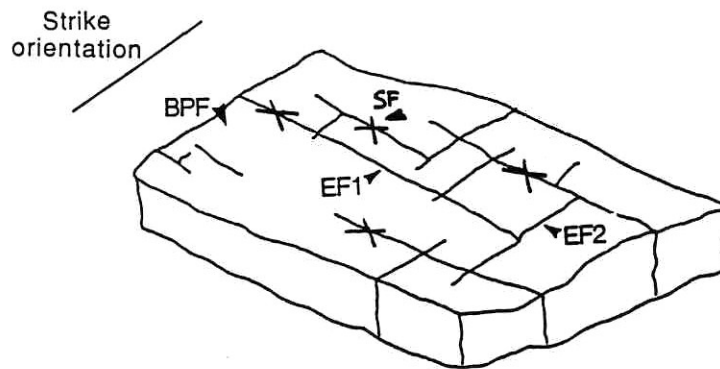


Figure 3. Schematic diagram of the fracture surfaces observed in the saprolite (modified from Dreier et al., 1987). Bedding plane fractures (BPFs) are the planes that define the upper and lower surfaces of the weathered shale layer shown. Extensional fractures (EFs), which are orthogonal to BPFs, are either perpendicular to strike (EF1) or parallel to strike (EF2). Shear fractures (SFs) form in sets which may or may not be at right angles to one another.

### *Mineralogy and porosity*

Mineralogical analyses conducted by Lee et al. (1991), Schreiber (1995), and Kooner et al., (1995) show that the predominant minerals in the  $< 2\mu\text{m}$  clay fraction of the weathered shale units are illite  $> 2:1$  randomly interstratified kaolinite:smectite  $>$  vermiculite  $>$  kaolinite  $>$  smectite, quartz, and plagioclase feldspar. In contrast the mineralogy of the weathered limestone units, that are now devoid of inorganic C and are massive clay lenses, is smectites  $>$  kaolinite  $>$  illite  $>$  interstratified 2:1  $>$  vermiculite  $>$  quartz. Clay minerals are heavily coated with Fe- and Mn-oxides, where 20-40 mg/g Fe and 0.5 to 1.0 mg/g Mn are not uncommon. Fracture coatings of calcite, goethite, amorphous Fe(III) and Mn(II)-oxides, and kaolinite were identified by Schreiber (1995) and Kooner et al., (1995). The carbonates contain low-Mg calcite, dolomite, and ferroan dolomite (Hatcher et al. 1992). The high clay content of the weathered saprolite and clay lenses creates a high porosity (30 to 50%), low permeability matrix that has an enormous impact on flow and transport characteristics since it serves as a source/sink during solute migration (Jardine et al., 1993a,b; 1999, 2001; Reddy et al., 1996).

## **Hydrology**

### *Vadose zone stormflow and recharge*

Clay infilling and higher bulk density material is commonplace in these Inceptisol soils. This scenario causes a large hydraulic conductivity contrast between the upper permeable soil and the underlying lower permeability saprolite creating a perched zone of saturation (stormflow zone) approximately 1.0 to 1.5 m below the surface. The majority of infiltrated stormflow water moves both parallel to the land surface (topography) and along dipping bedding planes (parallel or perpendicular to the topograph), ultimately discharging to local cross-cutting streams (Solomon et

al. 1992; Wilson et al., 1990, 1991a,b, 1993). Convergent subsurface lateral flow during storm events can produce mass flux rates on the time frame of tens of meters per hour, which is extremely rapid (Wilson et al., 1993). The remaining recharge migrates vertically through the soil profile to the water table zone (Mulholland et al., 1990; Solomon et al. 1992). The system is extremely hydrologically active since the Oak Ridge Reservation receives, on average, 1400 mm precipitation per year. Within the upper 8.5 m, recharge fluxes have been estimated at between 0.2 and 0.4 m/y with a mean vertical water velocity within the fractures of approximately 0.12 m/day based on CFC, tritium, and helium dating methods (Cook et al. 1996). There are also strong temporal effects on hydrologic processes determined by rainfall intensity and duration and by evapotranspiration over seasonal time scales. On 90% of the rainy days, daily rainfall is less than 30 mm and conversely, on 10% of all rainy days, daily rainfall is greater than 30 mm (Luxmoore and Huff, 1989). High intensity, short duration storms are commonplace in the summer months.

#### Transition zone groundwater flow

The majority of groundwater flux in the saturated zone is focused within an interval defined by the interface between the competent bedrock and overlying highly-weathered saprolite, commonly referred to as the "transition zone." This zone is generally defined as the interval between auger refusal and good core recovery by conventional rotary or cable tool methods. Characteristics of this zone are dense fractures and the relative absence of weathering products that contribute to poor core recovery and greater resistance to auger penetration. These characteristics also result in a significantly higher permeability as compared to both the overlying saprolite and underlying bedrock (Moline et al. 1998, Jardine et al., 1999a). The water table fluctuates from less than a meter near streams to three meters or more seasonally and during individual storm events. The transition zone tends to be saturated throughout most or all of the year and groundwater moves through this zone laterally in directions that are heavily influenced by fracture orientation and characteristics (Moline et al. 1998, Sanford and Solomon, 1998; Jardine et al., 1999a). Tracer tests in the shallow groundwater zone have demonstrated strike-preferential flow oblique to the average hydraulic gradient (Moline et al. 1998; Schreiber et al. 1999; Lee et al. 1992; Jardine et al., 1999a). Pumping tests conducted at two sites (Gierke et al. 1988; Lee et al. 1992) have demonstrated greater transmissivity along strike, and estimates of horizontal anisotropy based on the pump test range from 8:1 to 30:1, strike to dip.

#### Porosity and flow

Porosity within the matrix ranges from approximately 30-50% in the weathered saprolite (Jardine et al. 1988, 1993a,b; Wilson et al. 1992) to 3-15% in the underlying shallow bedrock (Dorsch et al. 1996). The effective porosity is likely to be significantly lower, however, based on modeling of tracer tests at both laboratory (Koch et al. 1999) and field scales. The fitting of tracer breakthrough curves requires an effective porosity in the saprolite closer to 20%, meaning that one third to one half of the total pore volume in the matrix is isolated and therefore inaccessible to advective and diffusive transport (see Jardine et al. 1988; Reedy et al., 1996). Fracture porosity is generally less than 5 to 10 % (Wilson and Luxmoore, 1988; Solomon et al. 1992; Reedy et al., 1996) yet is able to carry greater than 95 % of saturated groundwater flux. The matrix on the other hand, contains 90-95% of the total porosity, yet its permeability is orders of magnitude lower than fractures. Thus

fractures serve as conduits for preferential solute movement and the matrix serves as a high capacity source and sink for contaminants (Jardine et al., 1999a; 2001, 2002; Mayes et al., 2003).

Bulk hydraulic conductivity in these geologic materials varies over seven orders of magnitude ( $10^{-2}$ - $10^{-9}$  cm/s), depending on the presence or absence of fractures within the volume of influence and their characteristics (e.g., aperture, spacing, connectivity), (Wilson and Luxmoore 1988; Wilson et al. 1989; Wilson et al. 1992). The low end most likely represents the unfractured matrix and clay lense material that is often without structure. In general, hydraulic conductivity decreases with depth (Wilson and Luxmoore, 1988; Solomon et al. 1992). Storativities within the Nolichucky Shale bedrock range from  $1 \times 10^{-3}$  to  $5 \times 10^{-4}$  based on analysis of pumping test results using a variety of approaches (Gierke et al. 1988).

### Nonequilibrium processes

Since the subsurface media on the ORR is conducive to extreme preferential flow, physical, geochemical, and hydraulic nonequilibrium conditions between fractures and the surrounding soil matrix is commonplace (Reddy et al., 1996; Gwo et al., 1995; Jardine et al., 2001). Two processes contribute significantly to retardation of solute transport and the storage of solute mass in the matrix: sorption and matrix diffusion. High clay content within the weathered matrix coupled with high porosity and small pore size impart a large surface area for sorption of reactive solutes within the matrix and, secondarily, on fracture surfaces. In addition, these same characteristics result in a large, relatively immobile volume of pore water that acts as a reservoir for storage of solutes that diffuse into the matrix through the fracture walls (Fig. 4). The result is a significant slowing of the transport rates and the creation of secondary sources within the matrix that can and do release solutes over long periods of time. Because fracture flow rates are high, mass can be transported rapidly through preferred fracture flow pathways. This is particularly true of colloids and bacteria that reside only in the fractures due to size exclusion from the matrix. However, the overall mass flux may be low because of the low overall fracture porosity and, in the case of solutes, because of mass transfer into the matrix pores and onto solid surfaces.



### Fractures

Constitute < 5 –10 % of total porosity, yet are able to carry > 95% of saturated groundwater flux.

Serve as conduits for preferential contaminant migration.

### Matrix

Contain > 90-95% of total porosity; however, permeability is orders of magnitude lower than fracture.

Serve as high capacity source and sinks for contaminants.

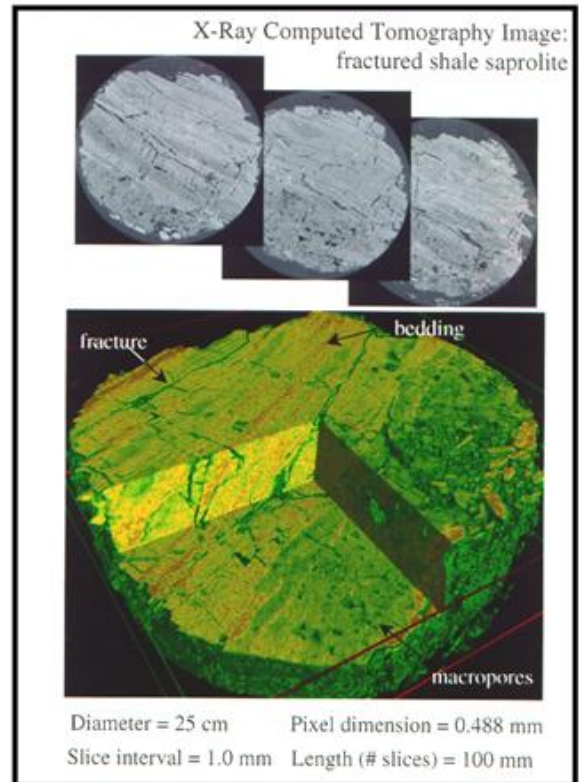


Figure 4. A close-up view of the FRC structured saprolite showing fracture densities on the cm scale. Highly interconnected fractures surround low permeability, high porosity matrix blocks creating a media that is conducive to preferential flow coupled with matrix diffusion. Also shown, is an x-ray computed tomography image of an undisturbed saprolite core showing density contrast between fractures and matrix in a 3-dimensional profile.

### Multipore region flow and transport

Functional relationships between water content ( $\theta$ ), pressure head ( $h$ ), and hydraulic conductivity ( $K$ ) suggest that the soil behaves as a three-region media consisting of macro-, meso-, and micropores (Wilson et al., 1992). Macro- and mesopores are conceptualized as primary and secondary fractures, and micropores as the soil matrix. The three region conceptualization of the fractured, weathered shales is supported by field measurements of Wilson and Luxmoore (1988) who showed mesopore convergent flow into macropores with subsequent bypass of the soil matrix (Fig. 5). Each pore region can be conceived as having its own flow and transport properties where mass exchange between the three domain occurs via advective and diffusive transfer. Hydraulic and concentration nonequilibrium between the different pore domains drives the rate of advective and diffusive mass transfer, respectively (Gwo et al., 1995; 1996, 1998).

The transport behavior described above has been demonstrated in laboratory tests in undisturbed cores (Sanford et al. 1996; Jardine et al. 1988, 1993a,b; Reedy et al. 1996; Moline et al. 1997;

Mayes et al., 2003) as well as field-scale tracer tests conducted at the background area (Lee et al. 1992; Moline et al. 1998; Sanford and Solomon 1998) and similar sites on the Oak Ridge Reservation (Wilson et al. 1993; Jardine et al. 1999a, 2003). Cook et al. (1996) discuss the implications of the matrix diffusion process on the use of environmental tracers for dating the age of groundwater and interpretation of the data for inferring such parameters as recharge rates and vertical groundwater velocities.

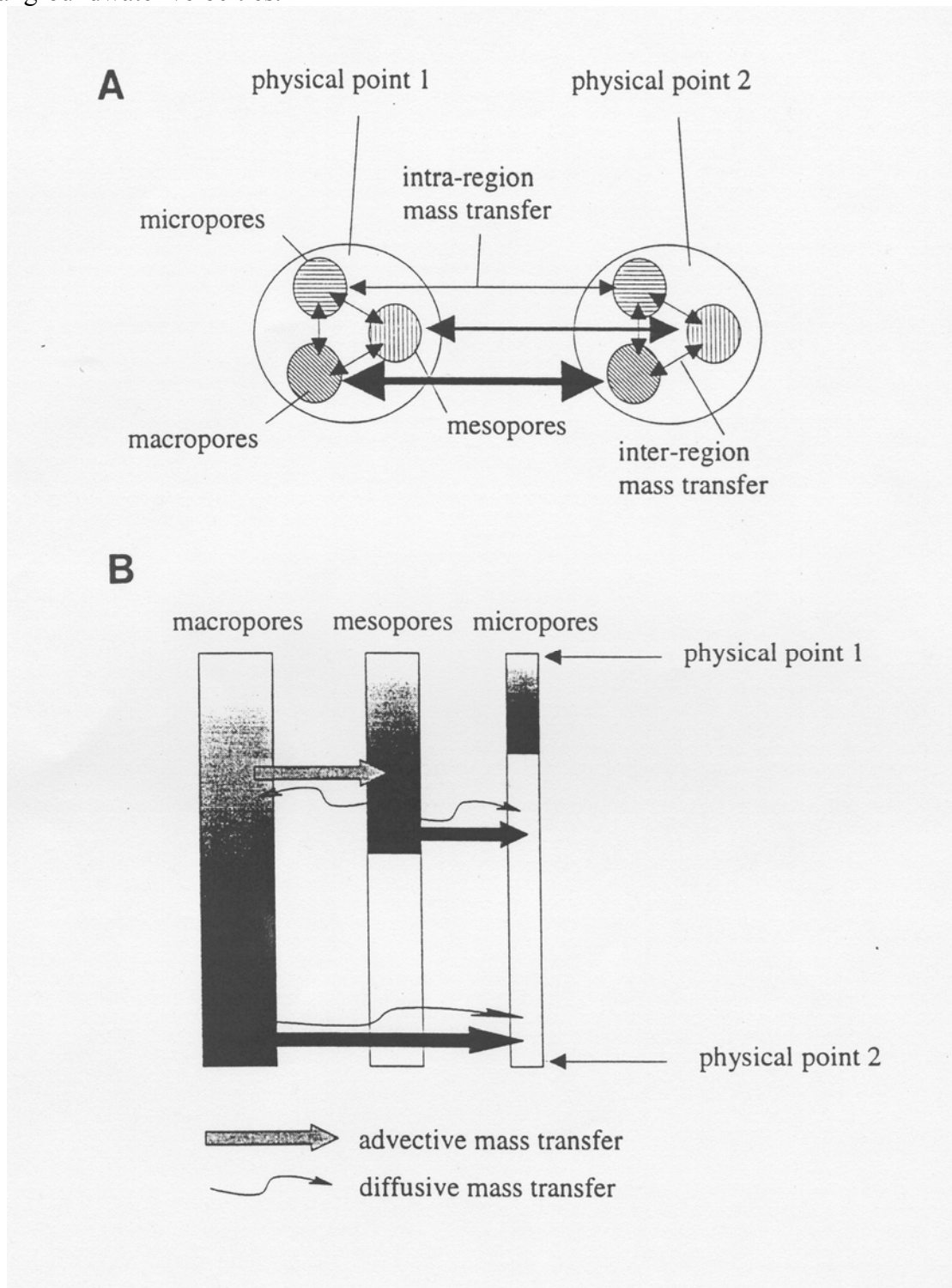




Figure 5 An example of the triple-porosity, triple-permeability multiregion flow and transport concept. (a) The REV (large circle) at two physical points consists of three pore regions. Intra-region flow and transport is indicated by lines between large circles (REVs) and inter-region transfer is depicted by lines within each large circle (REV). (b) Both advective and diffusive mass transfer may occur in parallel or counter to each other.

## Geochemistry

### Stormflow and groundwater chemistry

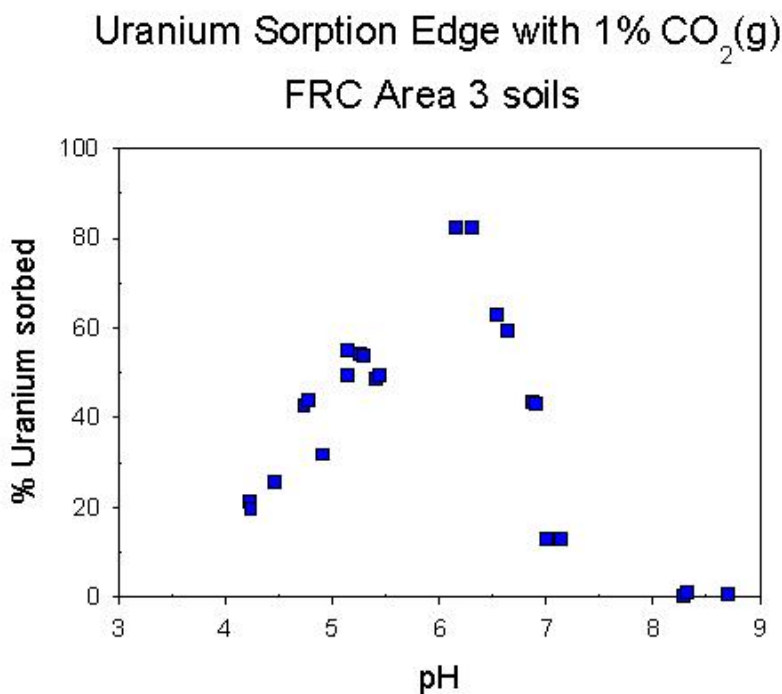
Extensive sampling of water chemistry within the stormflow zone, vadose zone, and shallow groundwater zone was conducted at the experimental field sites instrumented in the shallow unconsolidated zone and bedrock within the background area from 1995 through 1998. Sampling initially consisted of two separate sampling events conducted during a wet seasonal (January 1995) and dry season (July 1995) period within the multilevel wells at one of the field research sites (Schreiber 1995; Schreiber et al. 1999). These data demonstrated that the shallow groundwater at the field site is neutral to slightly alkaline (pH 7-8) and can be divided into four major water types: Ca-HCO<sub>3</sub>, Ca-Na-HCO<sub>3</sub>, Na-Ca-HCO<sub>3</sub>, and Na-Ca-HCO<sub>3</sub>-SO<sub>4</sub> waters.

A follow-on investigation was conducted that included intense sampling of stormflow tubes, vadose zone multilevel samplers, and numerous multilevel and standard wells for ion chemistry, stable isotopes, helium, and CFCs (Van der Hoven et al. 1997). These sampling events were conducted monthly for a period of 14 months from November 1996 through January 1998 to capture seasonal changes in water chemistry. In addition, storm-event sampling was conducted using a subset of the well network to measure high frequency changes in groundwater chemistry and during these sampling events precipitation and water from a nearby cross-cutting stream were also sampled.

### Interfacial geochemical reactions

The fractured, weathered shales are slightly acidic (e.g. pH 4.5-6.0) with typical cation exchange capacities of 15-20 cmol<sup>+</sup> kg<sup>-1</sup>. The <2μm clay fraction is predominately illite with lesser quantities of 2:1 interstratified material and vermiculite (Kooner et al., 1995). Carbonates are completely weathered from the upper several meters of soil and most of the fracture pathways and matrix blocks are coated with amorphous Fe- and Mn-oxides. The diverse mineralogy results in a highly reactive solid phase that can significantly alter the geochemical behavior and transport of solutes. Solute sorption, oxidation/reduction, and precipitation/dissolution reactions are commonplace within these soils (Jardine et al., 1988; 1993a,b; 1999b; Mayes et al., 2000). Cationic contaminants are often retarded by electrostatic or complexation reactions with the solid phase. Electrostatic bonds are not nearly as effective as inner and outer sphere complexation bonds for retaining contaminants. The uranyl cation is often sorbed by weaker electrostatic bonds on clay minerals or disordered outer and inner sphere complexation mechanisms allowing it to be an exchangeable cation in the FRC sediments. However, there are numerous situations where high levels of solid phase phosphate scavenge U(VI) from solution forming very strong inner-sphere complexes that are fairly nonlabile thus essentially immobilizing U on the solid phase. Soil pH is also a very important factor controlling retardation mechanisms by these soils. Changes in pH will cause changes in the surface charge of the FRC soil due to its amphoteric nature as well as possible

changes to the speciation of contaminants in the system. For example, an increase in pH will cause the solid phase of variably charged minerals such as Fe-oxides to become more negative and thus more accommodating for cation adsorption. Conversely, an increase in pH above 6.5 will cause the formation of  $\text{U-CO}_3$  anionic species that have little to no reactivity with the solid phase and are free to migrate in the groundwater (Fig. 6). The redox environment and the presence of redox reactive minerals and solids (e.g. Mn-oxides and organic matter) also impact contaminant transport at the FRC. Mn-oxides are powerful oxidants and reductants and can change the valence state of numerous cations and anions in the subsurface system. Cations such as Cr(III), Co(II), and U(IV) can be readily oxidized by Mn-oxides. The change in redox state can be significant as is witnessed with Cr dynamics, where the oxidation reaction converts a cationic Cr(III) species to an anionic, more mobile and toxic Cr(VI) species. Solid and solution phase organic matter also can act as strong reductants which can alter the redox state of contaminants. For example, organic matter is extremely effective at reducing Cr(VI) to sparingly soluble Cr(III) thereby decreasing its mobility at the FRC.



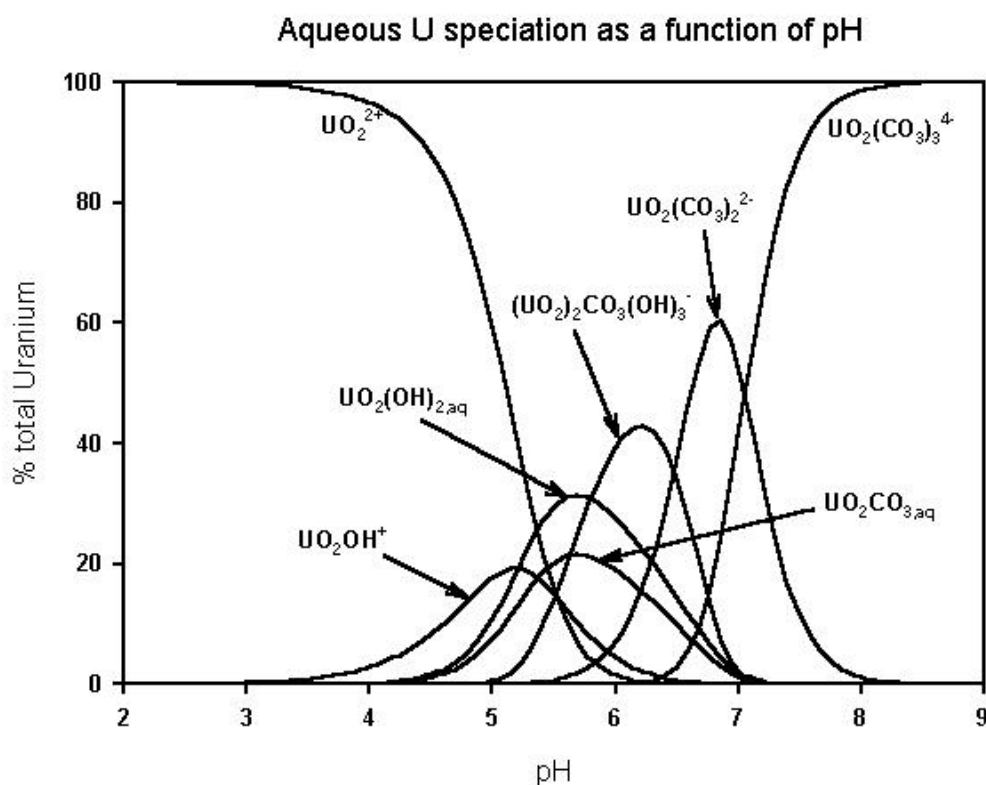


Figure 6. (a) Uranium pH sorption edge at 1%  $\text{CO}_2$  on Oak Ridge FRC soil acquired from a preferential flow zone located 42 feet in depth at Area 3. Uranium exhibits classic cationic sorption up to pH 6.2 and anionic repulsion above pH 6.2. The latter is the result of the formation of various U- $\text{CO}_3$  species (b).

## Microbiology

Microbial clonal libraries of the SSU rRNA gene have been constructed from groundwater samples taken at the FRC background site (Table 2). The bacterial community structure was diverse at the background site, and representatives of at least seven bacterial divisions or subdivisions were detected, including  $\alpha$ -,  $\beta$ -,  $\gamma$ -,  $\delta$ -Proteobacteria, high G+C Gram-positive bacteria, low G+C Gram-positive bacteria, Verrucromicrobia, and Acidobacteria (Fig. 7). Almost all the unique OTUs from the FW-300 sample appeared to be unique to the background site (74/79), and PCA indicated that the background microbial community was markedly different from those at the contaminated sites. LIBSHUFF analysis also indicated that the clonal library from the background sample was drastically different than the contaminated sites, and these results suggested that the contaminant load had altered the microbial communities (discussed below). Bacterial isolates ( $n=68$ ) classified as  $\beta$ - or  $\gamma$ -Proteobacteria, high G+C Gram-positive or low G+C Gram-positive were obtained from the background sample, and some of the isolates had less than 95% sequence identity with previously observed microorganisms. Comparing the background microbial community structure

with those of the contaminated sites (discussed below) suggested that contaminants (i.e., nitrate, uranium, nickel) and pH levels impacted both the cultivated and as-yet uncultivated bacterial communities at the respective sites. The apparent alterations of the microbial community composition at the disturbed sites suggested that the contamination has had a drastic affect on microbial community structure and suggested a selection for microorganisms able to tolerate increased levels of nitrate and heavy metals.

Table 2. Clonal libraries from FRC Background Area

| Groundwater sample  | Genera detected via SSU rRNA clonal libraries   |
|---------------------|---|
| FW-300 (background) | <i>Acinetobacter</i> spp., <i>Stenotrophomonas</i> spp., <i>Legionella</i> spp., <i>Duganella</i> spp., <i>Leptothrix</i> spp., <i>Propionivibrio</i> spp., <i>Pseudomonas</i> spp., <i>Sphingomonas</i> spp., <i>Bdellovibrio</i> spp. |

Matthew W. Fields, Tingfen Yan, Sung-Keun Rhee, Susan L. Carroll, and Jizhong Zhou

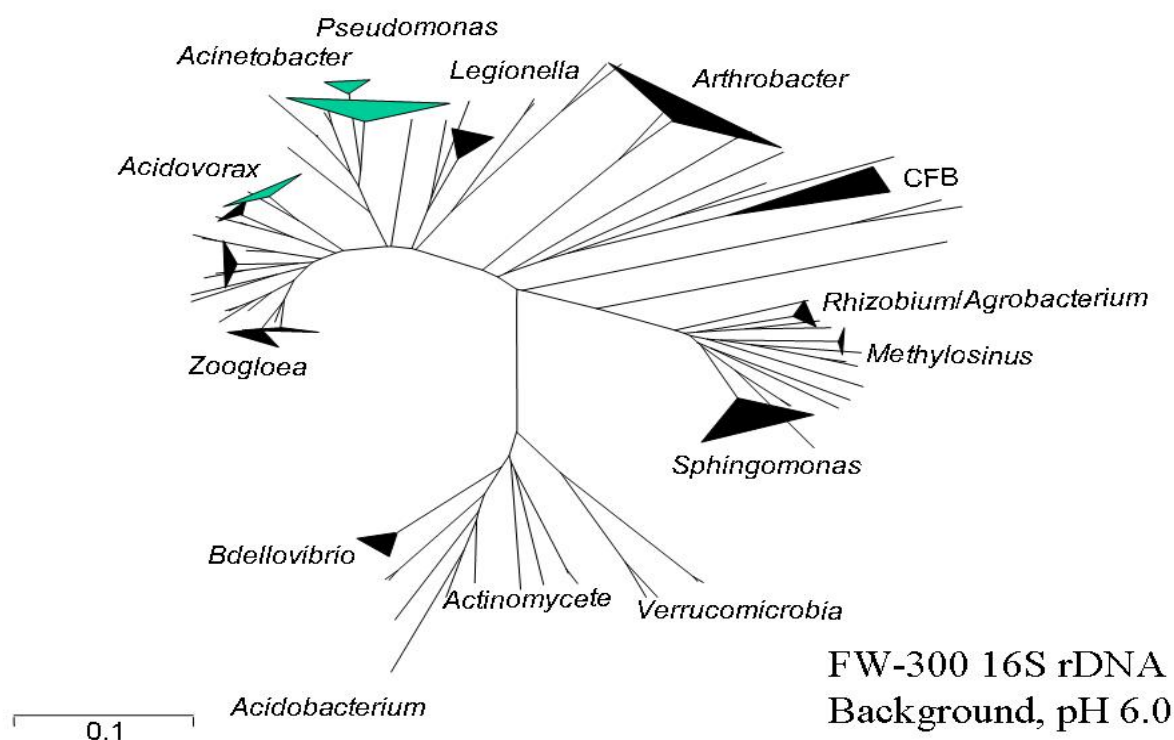


Figure 7. Phylogenetic tree of microorganisms isolated from well FW-300 of the Oak Ridge FRC background site. Such trees describe how diverse and related the various isolates are for a particular environmental setting.

### 3. OAK RIDGE FRC CONTAMINATED AREA

#### General Area Description

This section summarizes the characteristics of the Field Research Center (FRC) contaminated area which encompasses five field research areas, each of which is discussed in detail below. The 98 hectare contaminated area (Fig. 1) is located in Bear Creek Valley (BCV) just west of the main Y-12 industrialized plant area. The majority of the area is open although there are some wooded areas. Bear Creek flows down the middle of the area adjacent to Bear Creek Road. The flow in Bear Creek is supplemented by small tributaries originating on the southern slope of Pine Ridge, and by springs emanating mainly from the base of Chestnut Ridge. The tributaries convey shallow groundwater that has discharged to the surface and stormflow. In its upper reaches, Bear Creek follows a relatively straight course along the geologic strike close to the contact between the Maynardville Limestone and Nolichucky Shale. The original channel on the west side of the S-3 Ponds was filled with rubble during pond construction and rerouted to its present location (Law Engineering, 1983).

Major facilities that fall within the area include the S-3 Ponds, which is currently covered with an asphalt parking lot, the West End Treatment Facility (WETF), and the S-3 Ponds Pathway 1 and Pathway 2 reactive barrier demonstration projects (Fig. 8). Dozens of single and paired wells have been installed at the two reactive barriers sites and within the various research areas within the contaminated FRC. These wells, and dozens of other wells installed in the area by the Y-12 Groundwater Protection Program, are available for research purposes.

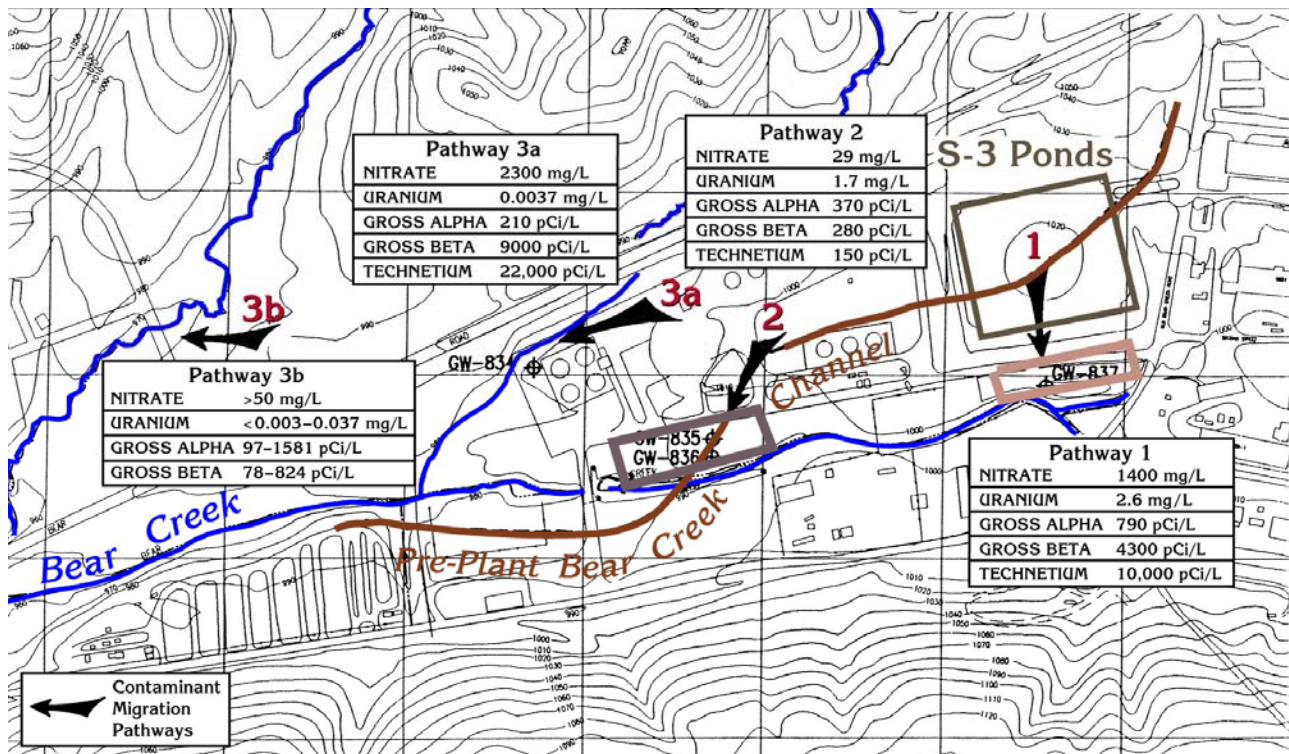


Figure 8. Primary contaminant transport pathways around the former S-3 waste disposal ponds.

## **Waste Disposal Units**

Beginning in the late 1940s and continuing into the early 1980's, hazardous and radioactive materials from Y-12 Plant operations have been disposed at various sites in BCV (USDOE 1997). The principal waste areas and contaminant sources in BCV are located in the upper 3.5-km of the valley on the outcrop of the Nolichucky Shale. Of these waste disposal units, the S-3 Ponds and Boneyard/Burnyard (BY/BY) are the primary contributors of contamination to the area.

The former S-3 Waste Disposal Ponds consisted of four unlined surface impoundments that were constructed in 1951. They received liquid nitric acid and uranium-bearing wastes via a pipeline at a rate of approximately 10 million liters/year until 1983. The Ponds were unlined and approximately 122-m × 122-m in dimension and 5.2-m deep. Infiltration was the primary release mechanism to soils and groundwater. In 1984, attempts were made to neutralized and bionitrified the S3 ponds. The ponds were subsequently closed and capped in 1988. The site is currently a large asphalt parking lot.

The BY/BY is not located within the FRC contaminated area but is one of the primary sources of uranium contamination in the Maynardville limestone. The BY/BY includes the 1) boneyard, which consisted of unlined shallow trenches that were used to dispose of construction debris and to burn magnesium chips and wood; 2) burnyard, which was used from 1943 to 1968, and received wastes, metal shavings, solvents, oils, and laboratory chemicals that were burned in two unlined trenches; and 3) Hazardous Chemical Disposal Area (HCDA), which was built over the burnyard and handled compressed gas cylinders and reactive chemicals. The residues from the cylinders and reactive chemicals were placed in a small, unlined pit. Although the HCDA has been capped, the rest of the BY/BY has not been capped.

## **Geology**

### Bedrock

The boundary of the western portion of the FRC contaminated area was selected to include the S-3 Ponds groundwater plume in the Nolichucky Shale. The eastern half of the area overlies the portion of the Maynardville Limestone that contains the co-mingled S-3 Ponds Plume and BY/BY uranium groundwater plume.

The geology of BCV displays an inclined layer-cake-style stratigraphy that is observed on a regional scale where limestone- and dolomite-dominated rock groups are interbedded with predominantly clastic shale groups, and on the scale of outcrops where clastic beds are interlayered with carbonate beds. The orientation of geologic units is parallel and coincident to the valleys and ridges. Three primary fracture sets have been identified parallel to bedding, perpendicular to bedding along strike, and vertical parallel to dip (Hatcher et al. 1992; Solomon et al. 1992; Fig. 3 and 9). Additional fracture sets may also exist, and local deformation may alter the orientation of the fracture sets relative to the regional structural grain. Fracture density ranges from about 15 to 30 fractures per meter based on rock coring and geophysical logging (Lee et al. 1992, Fig. 9).

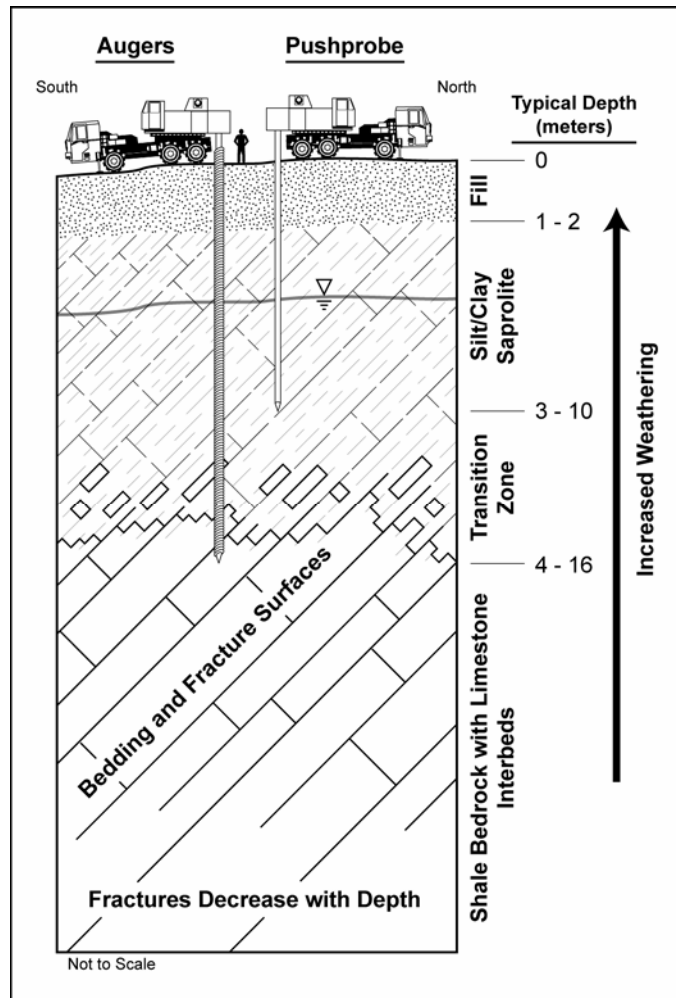


Figure 9. Schematic of a typical Oak Ridge FRC soil and bedrock profile showing the dramatic decrease in fracture density with depth.

Bear Creek Valley is underlain by rocks of three regionally important stratigraphic units: the Rome Formation, the Conasauga Group, and the Knox Group, that typically dip  $45^\circ$  to the southeast and have a geologic strike of N55E (Figs. 1, 2, and 10). All of these rocks were formed over 500 million years ago in the Cambrian geologic age. General descriptions of the stratigraphy of geological units on the Oak Ridge Reservation are provided in the BCV Remedial Investigation Report (USDOE 1997) and Hatcher et al. (1992). These units can be grouped into those that are mainly clastic (i.e., shales) and generally have lower permeability, and those that are mainly carbonates and are generally more permeable (Solomon et al. 1992).

The Rome Formation and the Conasauga Group crop out in BCV on Pine Ridge and dip to the southeast beneath BCV. The primary geologic units of interest that underlie the FRC contaminated area are the Maynardville Limestone (67 to 136-m thick) and Nolichucky Shale (190-m thick), both of which are subunits of the Conasauga Group. The Maynardville Limestone and Nolichucky Shale underlie both the contaminated and background areas (Fig. 1). With the exception of the Maynardville Limestone, the Conasauga Group is a sequence of shale, siltstone, and thin-bedded



limestone. Some formations, however, include laterally continuous limestone beds that can be several meters thick, and high permeability zones parallel to bedding planes may exist, especially where karstification has enlarged fractures in limestone beds. The Maynardville Limestone, the uppermost member of the Conasauga Group, is a massively bedded limestone and dolomite with fracturing and karstification. The Maynardville Limestone forms the floor of BCV and contains the channel of Bear Creek along most of the valley. The Nolichucky Shale is located just up slope and stratigraphically lower than the Maynardville Limestone. The Knox Group (i.e., Copper Ridge Dolomite) underlies and forms Chestnut Ridge, the southern boundary of BCV.

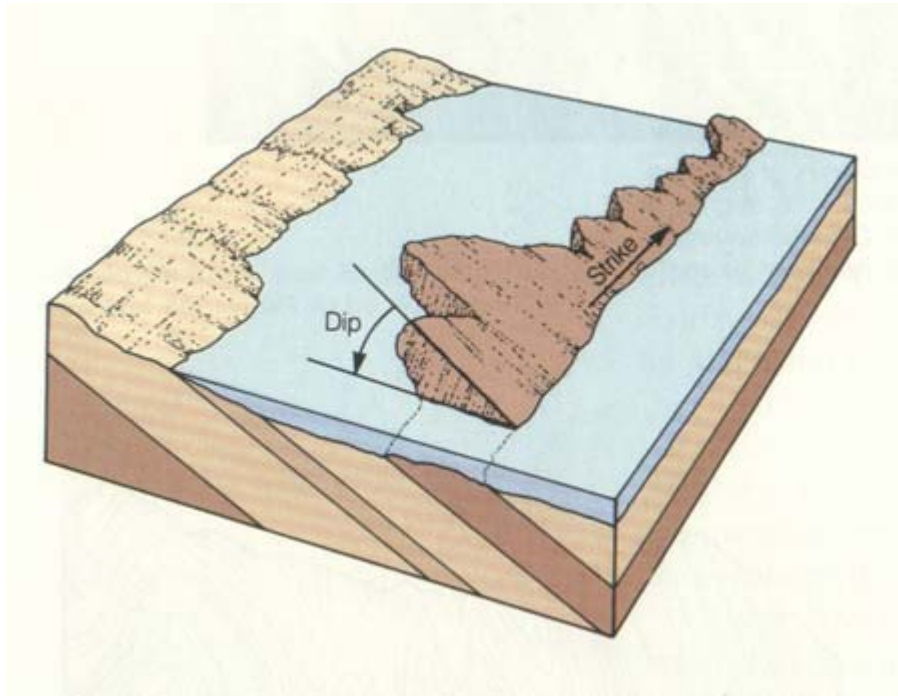


Figure 10. Schematic showing the direction of dip and strike for a layered media

## Porosity

The primary porosity of the rocks underlying the area is low, typically less than 2% in the Maynardville Limestone and approximately 10% in the Nolichucky Shales (Dorsch et al. 1996; Goldstrand 1995). The porosity of the residuum is typically 30 to 50 percent. Diagenesis, fracturing, and in the case of the carbonates, solution weathering (i.e., karstification) of bedrock have resulted in secondary porosity and increased permeability through which most fluid movement occurs (Solomon et al. 1992). Shevenell and Beauchamp (1994) have shown that the occurrence of cavities in the Maynardville Limestone decreases significantly below a depth of approximately 23-m. Below a depth of 23-m, water bearing zones are generally associated with fractures. Cavities are generally filled with silt and range in size from <0.3-m to >3-m, although, over 70% of cavities are <1.2-m.

## 2 Overlying saprolites



Overlying the bedrock on the Oak Ridge Reservation is unconsolidated material that consists of weathered bedrock (referred to as residuum or saprolite, (Fig. 2), man-made fill, alluvium, and colluvium (Fig. 9). Silty and clayey residuum comprises a majority of the unconsolidated material in this area. The depths to unweathered bedrock differ throughout the Oak Ridge Reservation because of the varying thicknesses of fill and alluvium, and the particular weathering characteristics of the bedrock units. The total thickness of these materials typically ranges from 3 to 15-m (Hoos and Bailey 1986). The thickness of residuum overlying the Nolichucky shale within the contaminated area is typically between 5 and 10-m thick. This material is the primary target for in situ sampling and research. The average thickness of residuum overlying the Maynardville Limestone is typically less than 3-m. In between the unconsolidated residuum and competent bedrock is a transition zone of weathered fractured bedrock.

## **Hydrology**

### Recharge

The contaminated area receives an average of 137 cm of precipitation per year, much of it occurring in the winter months (Fig. 11). As much as 50% of the infiltrating precipitation results in groundwater and surface water recharge (10 to 40%, respectively). The hydrogeology of BCV differs significantly between the mainly clastic formations (i.e. the Nolichucky Shale) and mainly carbonate formations (i.e., the Maynardville Limestone). In BCV, the contact between the Maynardville Limestone and the Nolichucky Shale roughly corresponds to the axis of the valley and marks a major transition from predominantly lower permeability clastic formations to higher permeability carbonate dominant formations. Groundwater in the clastic formations generally migrates along-strike in the unconsolidated residuum, transition zone and/or bedrock until eventually discharging to a tributary of Bear Creek. This surface water can enter the Maynardville groundwater system through losing sections of Bear Creek.

### General flow orientation

The orientations of well-connected fractures or solution conduits are predominantly parallel to bedding planes (i.e., geological strike, Fig. 10) and enhance the effect of anisotropy caused by layering. Remnants of this bedding plane fracturing are also present in the unconsolidated zone. This results in dominance of strike-parallel groundwater flow paths in both the unconsolidated zone and bedrock. Fracture aperture width generally decreases with depth in all formations and thus restricts the depth of active groundwater circulation. Active (or open) fractures occur at greater depths in the Knox Group and Maynardville Limestone than in the shale members of the Conasauga Group, and therefore, active groundwater circulation is deeper in these carbonate formations. Fracture densities in the near surface saprolites are in the range of 200 fractures per meter (Dreier et al., 1987) versus fracture densities of 5 fractures per meter in the more consolidated bedrock (Lemiske et al., personal communication, ORNL, 1995).

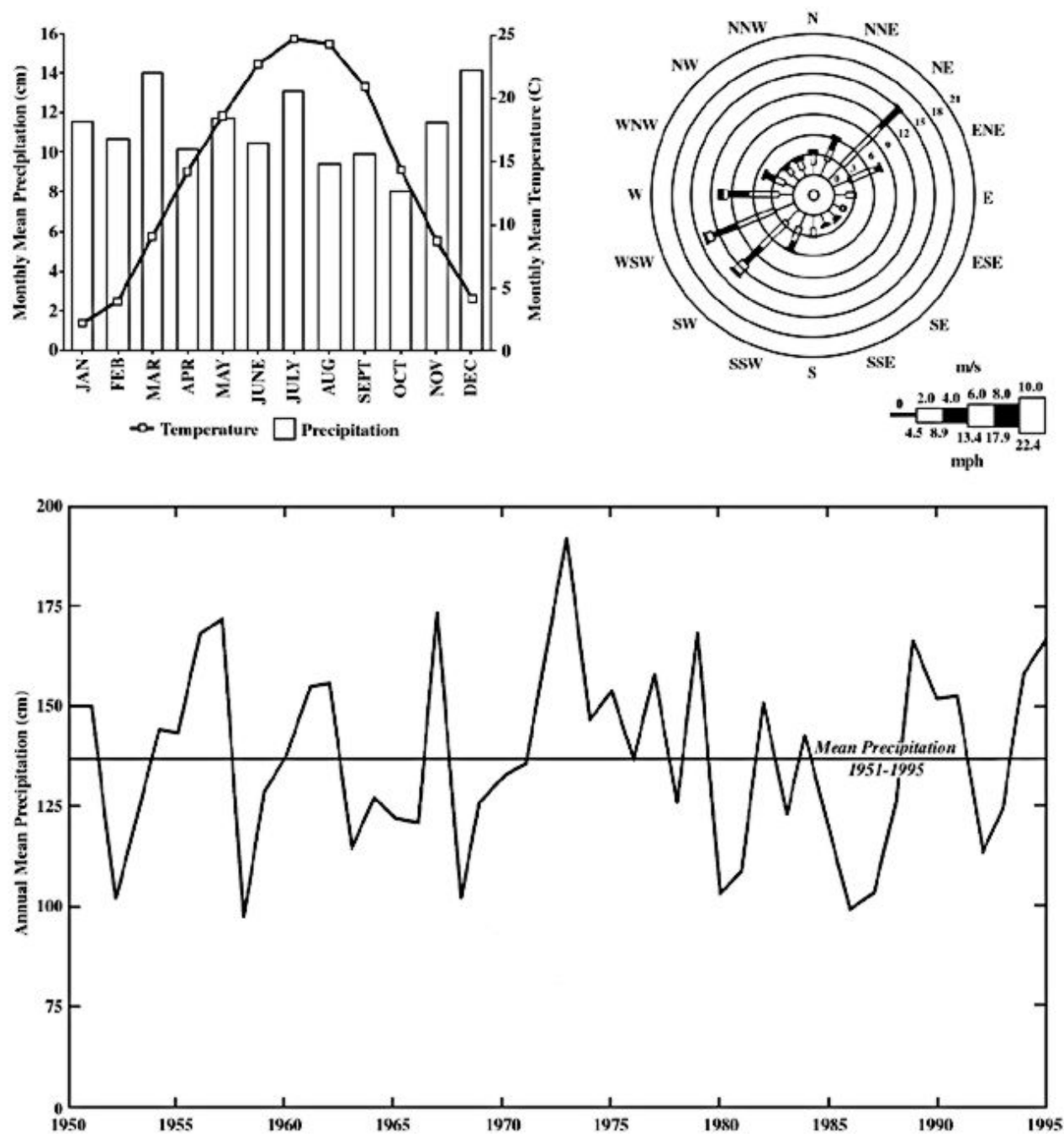


Figure 11. Climatological data from the Oak Ridge Reservation

### Groundwater Flow in the Unconsolidated Zone and Nolichucky Shales

Saturated flow in the shallow interval is oriented predominantly along geological strike, whereas unsaturated flow is influenced by local topography and dipping beds with discharge occurring at Bear Creek and tributaries to Bear Creek. Geochemistry indicates that greater groundwater residence times and, thus, slower flow generally occur below 30-m in the intermediate interval.

However, the distribution of contaminant plumes in BCV indicates that more rapid flow than predicted by major ion geochemistry may occur in an along-strike direction in preferential pathways in the intermediate interval and may occur up to 61-m in depth [nitrate from the S-3 Site has migrated approximately 1-km or more in the Nolichucky Shales since 1950].

A bromide tracer study test conducted in the unconsolidated zone at the Pathway 2 reactive barriers site (located within the contaminated Area 2) resulted in an average peak concentration arrival velocity of approximately 2-m/day. This value is consistent with point dilution measurements at Area 3 which suggested groundwater was moving 0.5 to 1 m / d near the transition zone. During the pathway 2 tracer test, however, a large mass of bromide remained in the vicinity of the injection well suggesting matrix diffusion has a significant impact on transport at this site. Pathway 2 is located near the location of an old Bear Creek stream channel and some springs in Bear Creek, therefore, transport rates in the residuum at other locations is expected to be as much as an order of magnitude less than this.

Pumping tests within the FRC contaminated area have provided estimated transmissivities of  $4.6 \times 10^{-6} \text{ m}^2/\text{s}$  and storage coefficients of  $1.4 \times 10^{-3}$  based on drawdown data in nearby wells. These values correspond favorably with data collected from other hydraulic testing conducted in the Nolichucky bedrock interval.

Multiregion flow and transport mechanisms are also the norm at the contaminated site as they are at the background site. High permeability fractures surround low permeability, high porosity matrix blocks on the cm scale, thus the media is not only conducive to significant preferential flow, it is also a source/sink for contaminants (Fig. 4). The large disparity between fracture and matrix permeabilities results in significant physical, hydraulic, and geochemical nonequilibrium which complicates conceptual and predictive modeling capabilities (Jardine et al., 2001). Secondary contaminant sources within the matrix are often ill-defined and therefore it is difficult to assess the risk associated with the off-site migration of the contaminants.

#### Groundwater Flow in the Maynardville Limestone

The Maynardville Limestone crops out along the southern side of the BCV floor and acts as a hydraulic drain for the valley. Flow in these formations is predominantly along strike and parallel to the maximum hydraulic gradient. The hydrostratigraphy in the carbonate formations is less defined than that in the Nolichucky Shale (Solomon et al. 1992). The definitions of shallow, intermediate, and deep regimes are not rigid and rely on cumulative evidence from fracture and cavity occurrence (Shevenell et al. 1992; Shevenell and Beauchamp 1994), and hydraulic and geochemical responses during storms and distribution of contamination (Shevenell 1994; USDOE 1997).

The shallow interval includes groundwater to approximately 30-m depth. The channel of Bear Creek can be considered conceptually as one of the main hydraulic conduits in this system. In this interval, groundwater flow is relatively rapid. Groundwater and contaminant transport in the residuum found over the Maynardville Limestone is less important than it is over the Nolichucky shales because the residuum over the Maynardville Limestone is thinner and transports a smaller percentage of groundwater flow. The intermediate interval occurs between approximately 30-m and

100-m depth. Solution cavities and solutionally enlarged fractures exist in the Maynardville Limestone in this interval and are probably well connected by fractures. Because of its depth, this zone is isolated from dilution effects seen in shallower zones. Thus, flow rates are probably slower than those in the shallow interval, but contaminant plumes are more persistent and extend farther along the valley. This zone constitutes an important contaminant transport pathway. In the deep interval [greater than 100-m depth], flow through fractures dominates groundwater movement, and flow zones become less frequent as fracture density decreases with depth.

Only one pumping test has been conducted in the Maynardville Limestone in BCV. The wells used to conduct this test are located in the background area. A transmissivity of  $1.2 \times 10^{-3} \text{ m}^2/\text{s}$  and storage coefficient of  $6.5 \times 10^{-4}$  were calculated from the drawdown data in nearby wells. The hydraulic conductivity of the Maynardville was estimated to be  $8.4 \times 10^{-3} \text{ cm/sec}$ .

## **Geochemistry**

### Soils

The residuum in the vicinity of the former S-3 Ponds is the primary source of soils contaminated with radionuclides and metals. The residuum is contaminated with metals (barium, copper, lead, mercury, nickel, vanadium and zinc), radionuclides (uranium, Tc-99, and Th-230), and organics (acetone, methylene chloride tetrachloroethylene, and toluene) above background concentrations. There are other contaminants detected above background levels but at a lower frequency and concentration. A detailed description of site specific contaminant concentrations is provided below.

The solid phase mineralogy at the contaminated sites is often heavily coated with Fe-oxides and therefore conducive to the sorption of both cations and anions. The amphoteric nature of the Fe-oxides often provides sufficient positive and negative charge to allow anions and cations to sorb. The permanent charge associated with solid phase clay minerals also provides a significant source of negative charge conducive to cation exchange. Near the contaminant source, the dominant anions on the solid phase will be sulfate and phosphate, while the dominant cations on the solid phase will be calcium, aluminum, and sodium. These solutes will dominate the surface exchange sites since their concentrations are high in solution and several of the solutes form strong bonds (i.e. phosphate, sulfate, aluminum).

Cationic contaminants will be retarded by electrostatic or complexation reactions with the solid phase relative to most anionic contaminants. Electrostatic bonds are not nearly as effective as inner and outer sphere complexation bonds for retaining contaminants. The uranyl cation is often sorbed by weaker electrostatic bonds on clay minerals or disordered outer and inner sphere complexation mechanisms allowing it to be an exchangeable cation in the FRC sediments. However, there are numerous situations where high levels of solid phase phosphate scavenge U(VI) from solution forming very strong inner-sphere complexes that are fairly nonlabile thus essentially immobilizing U on the solid phase. Soil pH is also a very important factor controlling retardation mechanisms by these soils. Changes in pH will cause changes in the surface charge of the FRC soil due to its amphoteric nature as well as possible changes to the speciation of contaminants in the system. For

example, an increase in pH will cause the solid phase of variably charged minerals such as Fe-oxides to become more negative and thus more accommodating for cation adsorption. Conversely, an increase in pH above 6.5 will cause the formation of  $\text{U-CO}_3$  anionic species that have little to no reactivity with the solid phase and are free to migrate in the groundwater (Fig. 6). The redox environment and the presence of redox reactive minerals and solids (e.g. Mn-oxides and organic matter) are expected to also impact contaminant transport at the FRC. Mn-oxides are powerful oxidants and reductants and can change the valence state of numerous cations and anions in the subsurface system. Cations such as Cr(III), Co(II), and U(IV) can be readily oxidized by Mn-oxides. The change in redox state can be significant as is witnessed with Cr dynamics, where the oxidation reaction converts a cationic Cr(III) species to an anionic, more mobile and toxic Cr(VI) species. Solid and solution phase organic matter also can act as strong reductants which can alter the redox state of contaminants. For example, organic matter is extremely effective at reducing Cr(VI) to sparingly soluble Cr(III) thereby decreasing its mobility at the FRC.

The geochemistry of aqueous and solid phase Al is also a very important consideration at the FRC, particularly near the source where the groundwater is most acidic and highly buffered. The low pH of the groundwater and high buffer capacity has resulted in significant dissolution of the solid phase minerals allowing Al to escape from the octahedral layer of phyllosilicate clays. Aluminum aqueous and solid phase geochemistry is extremely complex since this solute undergoes significant hydrolysis and polymerization above pH 4.0. Countless species of metastable polymers and precipitation products not only serve as a sink for co-precipitating metals, they also can result in enhanced contaminant mobility through Al-hydroxide colloid migration.

### Groundwater

Contaminants in the commingled S-3 Ponds and BY/BY plume include radionuclides (uranium, Th-230, and Tc-99), metals (strontium, cadmium, barium, boron, mercury, chromium), volatile organic contaminants (VOCs such as PCE and methylene chloride), nitrate, sulfate, and phosphate, and lesser amounts of other contaminants. Although, the S-3 Ponds site is a source of all of these contaminants, the BY/BY site has contributed primarily uranium and VOCs to the Maynardville Limestone. There are also some unknown sources of VOCs (PCE, TCE and DCE) in the Maynardville Limestone. A block diagram of the upper portion of Bear Creek Valley is shown in Figure 12.

The S-3 Ponds and BY/BY are located on top of the unconsolidated Nolichucky Shale, and historical waste discharges have contaminated shallow groundwater beneath the waste sites. Due to the high dissolved solids contents of the liquid wastes disposed at the S-3 Ponds site, contamination has migrated to depths as great as 130-m in the Nolichucky Shales. The S-3 ponds site is located on a groundwater divide so contamination has migrated to both the west and east. A block diagram showing a conceptual model of groundwater flow around the S-3 Ponds is shown in Fig. 13. The extent of nitrate, gross alpha (indicator of uranium) and gross beta (indicator of Tc-99) are shown on Figure 14. Nitrate is an excellent indicator of the extent of the S-3 Ponds plume. Most of the uranium (gross alpha) contamination detected in the Maynardville Limestone west of the BY/BY probably originated from the BY/BY. Typical groundwater quality of shallow piezometers installed at the FRC near the S-3 Ponds is summarized on Figure 15.

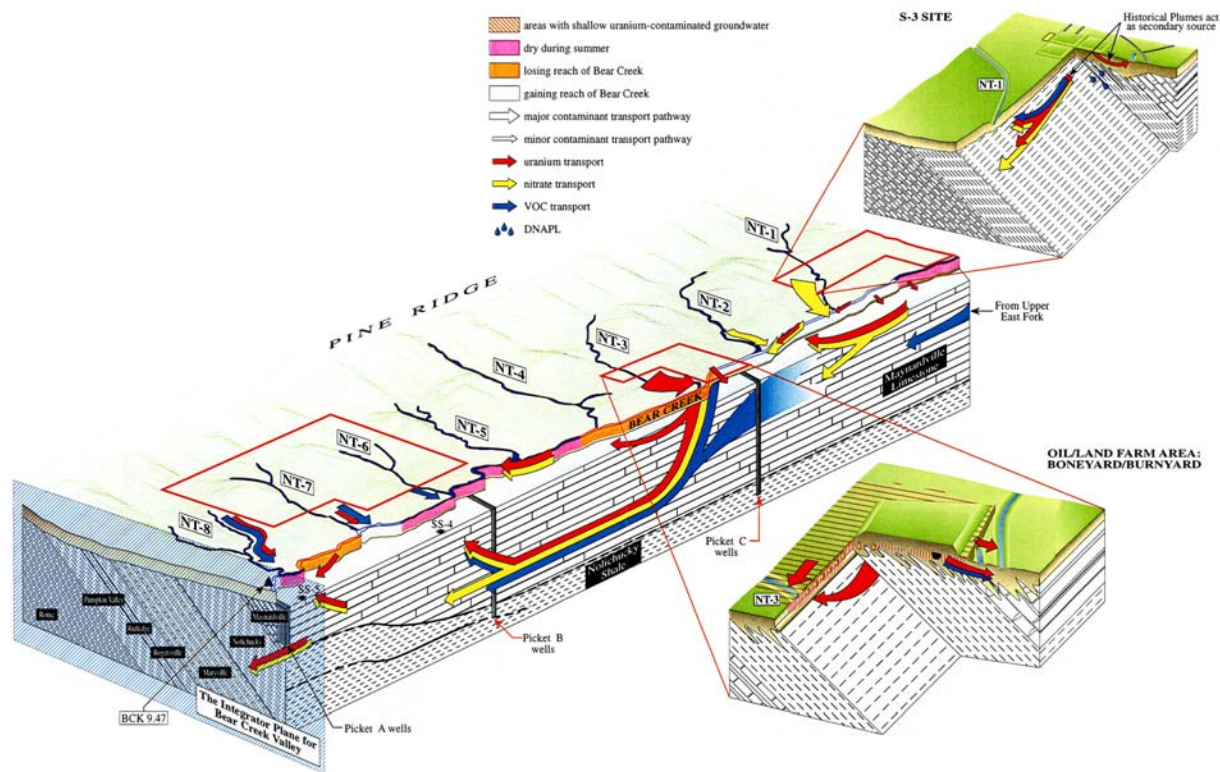


Figure 12. Conceptual rendering of contaminant transport away from the primary waste areas in Bear Creek Valley.

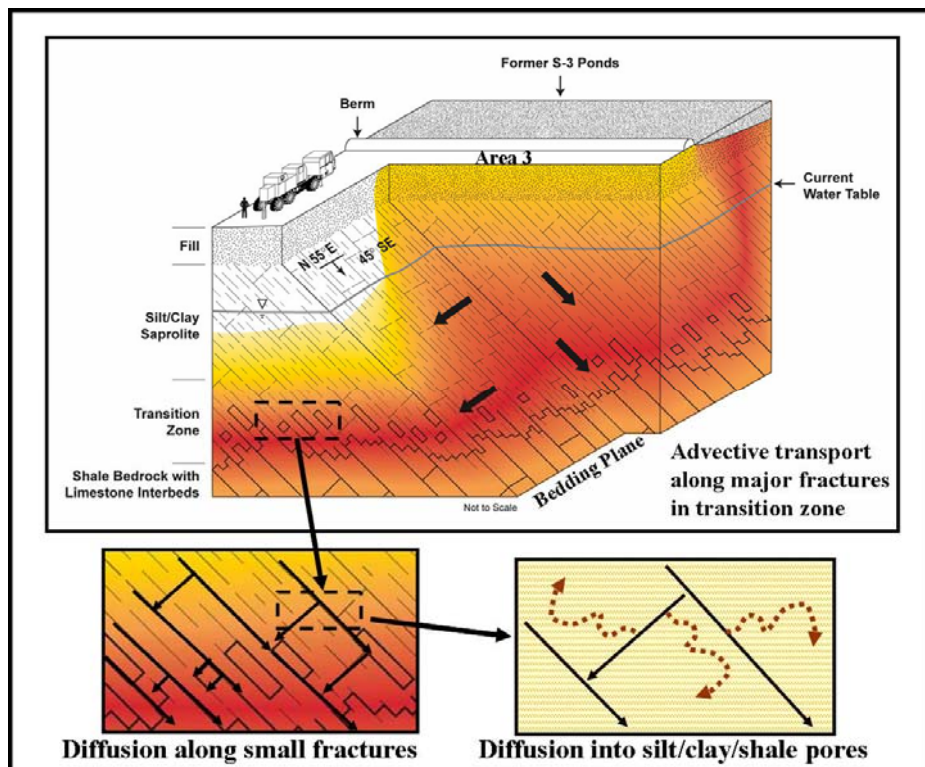


Figure 13. Conceptual rendering of contaminant transport in the vicinity of the S-3 Ponds

Background concentrations of dissolved oxygen in the residuum at the reactive barrier sites are generally 2 ppm but vary between 1 and 4 ppm, Eh varies between 100 and 300-mV, and pH varies between 5 and 6.5. Near the source, similar DO values are to be expected, however, the pH of the groundwater is strongly buffered at 3.5 to 3.8 to a depth of at least 47 feet where it begins to increase due to the increasing presence of carbonate-bearing minerals. The terminal electron acceptor process in the shallow residuum is likely driven by oxygen but there is also a significant potential for nitrate to be important to this process. Deep groundwater in the Nolichucky Shale and Maynardville Limestone can be anaerobic and have a negative Eh ( $< -250$ -mV). Under these groundwater conditions nitrate is likely to be the most important to the electron acceptor process.

Contaminants migrate away from the waste disposal units using the following pathways (Fig. 12). Contaminated shallow groundwater in the unconsolidated residuum and bedrock at sources on the Nolichucky Shale generally migrates along geological strike with local influences from topography, and discharges to tributaries or directly to Bear Creek causing Bear Creek to become contaminated. Contaminants in intermediate groundwater in the Nolichucky Shale also migrate through fractures along strike and discharge to tributaries (Fig. 10). After entering tributaries, contaminants migrate in surface water directly to Bear Creek. Bear Creek intermittently loses and gains water from groundwater in the Maynardville Limestone throughout the length of the valley. Losing reaches of Bear Creek cause groundwater contamination in the Maynardville Limestone (Fig. 12). Intermediate and deep groundwater in the Maynardville Limestone [30 to 90-m depth] constitutes less than 4 percent of water flowing along the valley. Concentrations of contaminants in this and in the deep groundwater pathway are not attenuated as rapidly as those in shallow groundwater, therefore, this pathway is an important source of long distance groundwater transport along BCV. Elevated nitrate concentrations and significant U have been detected to several hundred feet owing to rapid, unretarded movement through the Maynardville limestone.

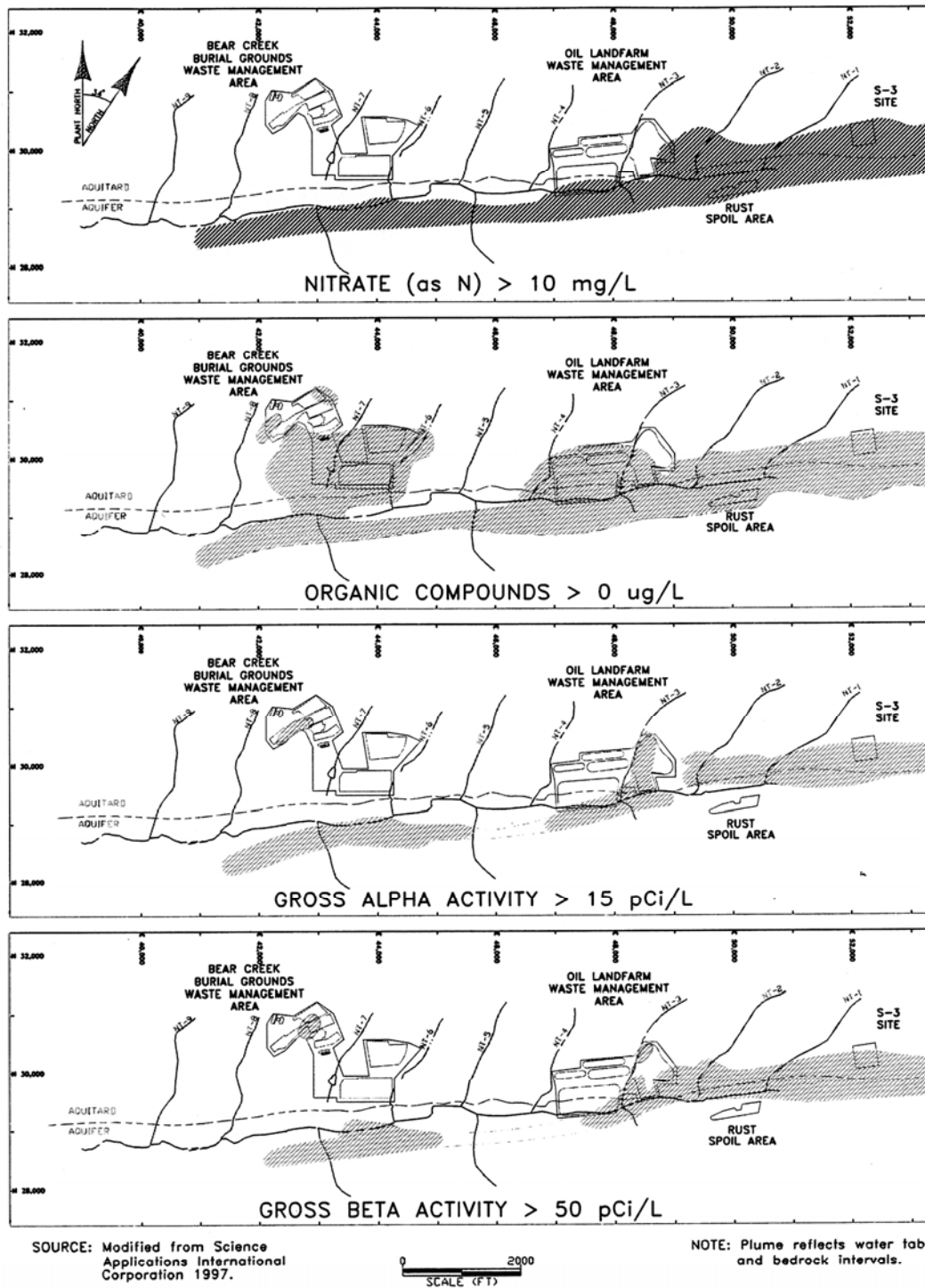
## Microbiology

Previous studies of microbial U(VI) reduction in sediments co-contaminated with nitrate have indicated that no net U(VI) reduction occurs until nitrate is reduced. Once nitrate is depleted, U(VI) and Fe(III) are reduced concurrently (Finneran et al., 2002a&b, Wielinga et al., 2000) presumably due to bioaggregate formation on the solid phase. Studies with sediments as well as pure cultures also suggest that once U(VI) is reduced, it may be remobilized via biotically or abiotically-catalyzed reactions with nitrate and denitrification intermediates (Finneran et al., 2002a; Senko et al., 2002). Thus denitrification and other microbially-mediated nitrogen transformations, intimately affect the fate of U in anoxic subsurface environments. Further, the presence of biogenic

Fe(II) will influence the reduction of U(VI) through direct abiotic U reduction and Fe(III)-oxide surface poisoning via readsorption.

The FRC subsurface is a challenging environment for organisms where conditions include: acidic pH, high nitrate concentrations in the presence of U, high concentrations of toxic metals (Al, Ni, Cu, Zn), and elevated concentrations of halogenated organic compounds. The most abundant electron acceptors available are nitrate and Fe(III) minerals. Iron(III) minerals in the FRC subsurface are mostly aluminosilicates and crystalline Fe oxides, but a substantial concentration of poorly crystalline Fe(III) is present and has been shown to be reduced. Viable counts of aerobes and anaerobes show lower numbers and decreased activity in contaminated FRC groundwater and sediments. As determined by both cultivation and noncultivation characterization methods, the abundance/ diversity of microorganisms in FRC sediments is dependent upon geochemical parameters such as pH and nitrate concentration. A number of PIs have shown that microbial consortia enriched from FRC sediment rapidly reduce U(VI) and grow with Fe(III) minerals as the sole electron acceptor (Kostka et al., 2002; Petrie et al., 2003, in press). At the FRC, field biostimulation experiments have indicated that microbial activity is limited by low pH and electron donor. Upon addition of electron donor and pH neutralization, extensive nitrate and metal reduction have been observed (Istok et al., 2004).





|   |             |                              |   |
|---|-------------|------------------------------|---|
| PREPARED FOR:<br><b>LOCKHEED MARTIN<br/>         ENERGY SYSTEMS, INC.</b> | LOCATION:   | Y-12 PLANT<br>OAK RIDGE, TN. | FIGURE 3.1.1-1<br><br>GROUNDWATER CONTAMINATION<br>IN THE BEAR CREEK HYDROGEOLOGIC REGIME |
|   | DOC NUMBER: | 97-D003                      |   |
|   | DWG ID.:    | 96-089                       |   |
|   | DATE:       | 5-20-97                      |   |
| PREPARED BY:<br><b>AJA TECHNICAL<br/>         SERVICES, INC.</b>          |             |                              |   |

Figure 14. Groundwater contaminant distribution in Bear Creek Valley.

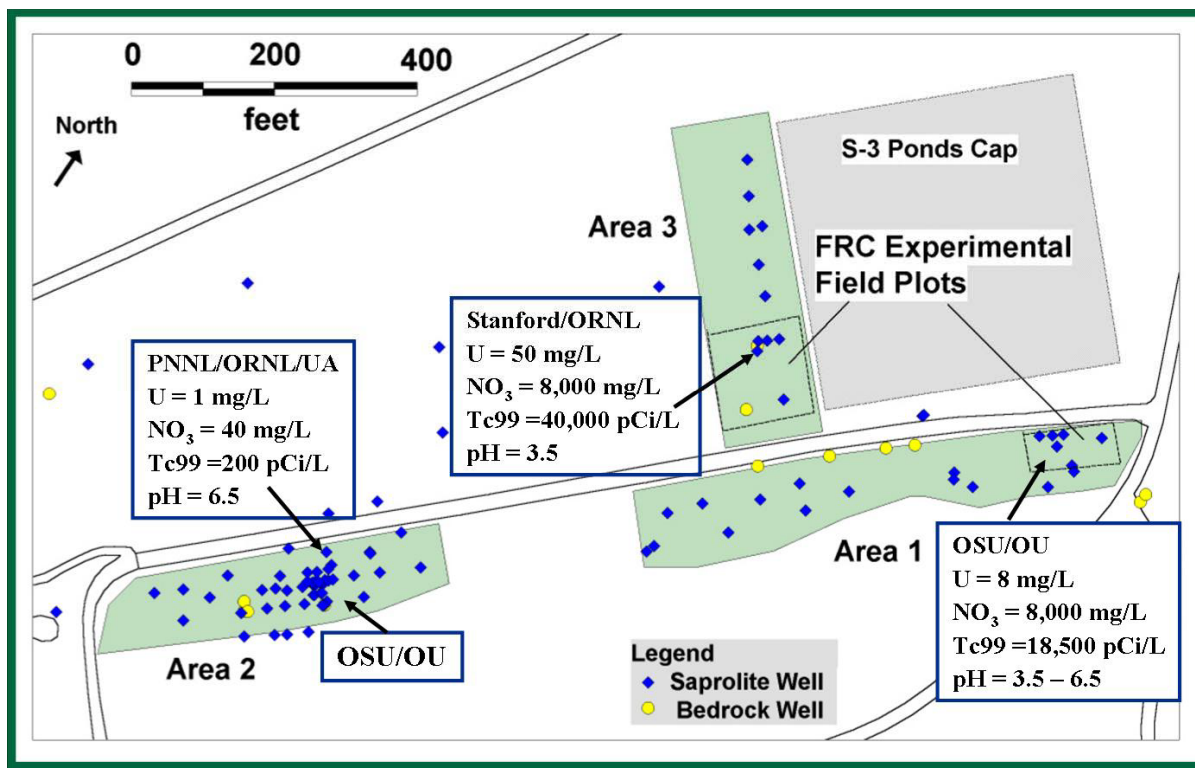


Figure 15. Location of research areas in the vicinity of the S-3 Ponds

### 3 HYDROLOGICAL, GEOCHEMICAL, AND MICROBIAL CHARACTERISTICS OF AREA 1

#### Geology and Hydrology

Area 1 is just south and down dip of the S-3 Ponds (Figure 15). A typical geologic profile at this field site would consist of about 1.5 meters of reworked fill and saprolite at the surface underlain by about 7 meters of intact saprolite with weathered shale bedrock below the saprolite. The saprolite consist of interbedded weathered shale and limestone, where the limestone has weathered to massive clay that is typically devoid of carbonate. Hydraulic conductivity of the shallow saprolite is fairly low (about 0.26 m/day) with maximum pumping rates of < 1 liter/minute. Hydraulic monitoring at the site indicates that the depth to groundwater is approximately 3.5 meters from the surface and the hydraulic gradient is low. Contaminants include all the contaminants generally associated with the S-3 Ponds groundwater plume (i.e., nitrate, technetium, uranium, volatile organic compounds and relatively high concentrations of other common anions and cations). Contaminants have migrated from the ponds to Area 1 via bed dipping fractures. Contaminant dispersal within Area 1, however, is along strike as this is the primary direction of groundwater flow in the saturated zone.

#### *Geochemistry*

Concentrations of contaminants in groundwater and soil from well to well are variable but tend to be fairly stable over time within individual wells. Contaminant concentrations are significantly lower than is typical of Area 3. Area 1 is down dip from the S-3 ponds which is not the preferred direction of groundwater movement under saturated conditions. Because Area 1 is down dip, contaminants must migrate across strike and this increases their variability and decreases their concentration. Deeper groundwater monitoring wells within Area 1 tend to have higher nitrate concentrations relative to shallow groundwater wells since the deeper wells are directly down dip from the ponds and contaminants can be preferentially transported along bedding plane fractures. Nitrate concentrations at the Area 1 field plot in groundwater range from 48 to 10,400 mg/l, uranium ranges from 0.01 to 7.5 mg/l, and technetium-99 ranges from 66 to 31,000 pCi/l. Wells with high uranium (e.g., >1 mg/l) tend to have high to moderate nitrate (>1,000 mg/l) and high technetium concentrations (>12,000 pCi/l). The pH of groundwater at Area 1 tends to be more acidic than Area 2 but ranges between 3.25 and 6.5 with dissolved oxygen content about 1-2 mg/L. Sulfate concentrations range between 219 mg/l and 1 mg/l, and chloride concentrations range between 22 and 760 mg/l. Aluminum can be as high as 620 mg/l and nickel is found at concentrations of 8.6 mg/l. Calcium, sodium, magnesium, and manganese are other metals detected at significant concentrations (>100 mg/l) at the site. Tetrachloroethylene (0.120 mg/l), acetone (0.230 mg/l), and some other volatile organic compounds (VOCs) are also detected in the groundwater of Area 1 field plot. As much as 375 mg/kg of uranium is associated with the solid phase material.

### Sediments

Microbial characterization of subsurface sediments at Area 1 has involved 16S rRNA gene sequences retrieved via direct DNA extractions on solid phase material before and after biostimulation (Kostka et al., 2004). It was found that a large diversity of 16S rRNA sequences from FRC sediment existed, including species from all subdivisions of the *Proteobacteria*, as well as low and high G+C Gram-positive species. Phylogenies which infer certain physiologies, such as nitrate reduction, metal reduction, dechlorination, and degradation of metal-chelator complexes and fuel hydrocarbons were identified (Kostka et al., 2004). Common clones detected from contaminated sediment were closely related to *Methylobacterium*, including a group of bacteria with the ability to degrade EDTA-metal complexes. After *in situ* biostimulation via push-pull tests conducted by Istok et al. 2004, clone libraries of contaminated sediments were dominated by the delta-*Proteobacteria*, which comprised 40% of all 16S rRNA gene sequences. Cloned sequences within the delta-*Proteobacteria* were all closely related to known dissimilatory Fe(III)-reducing bacteria that are members of the *Geobacteraceae* family or to *Anaeromyxobacter dehalogenans*. Subsurface sediments from the background site contained a lower diversity in retrieved sequences as compared to the contaminated and biostimulated clone libraries. Most retrieved sequences from the background site were either closely related to the beta-*Proteobacteria*, or were not closely related to any previously identified organisms.

Kostka et al., (2004) also selected groups of microorganisms identified earlier in Fe(III)-reducing enrichments from FRC sediment, *Geobacter sp.*, *Anaeromyxobacter sp.*, *Paenibacillus sp.*, and *Brevibacillus sp.*, for further study. These microbial groups were quantified *in situ* using an MPN-PCR technique before and after sediment biostimulation (push-pull activity experiments conducted in the field by Istok et al., 2004). Quantitative PCR revealed an increase in *Geobacter sp.* 16S rRNA sequences after biostimulation, suggesting that members of the *Geobacteraceae* are likely to be important in catalyzing metal reduction in contaminated FRC sediment. Evidence from the quantitative analysis corroborated information obtained from 16S rRNA gene clone libraries, indicating that members of the delta-*Proteobacteria*, including *Anaeromyxobacter dehalogenans*-type and *Geobacter*-type sequences, are important metal-reducing organisms in the FRC sediment.

Fe(III)- and U(VI)-reducing bacteria were enriched from the subsurface sediments of Area 1 at pH 4-5 and pH 7 (Petrie et al., 2003, in press). Iron(III) oxide was used as the sole electron acceptor for all enrichments, and carbon substrates included acetate, lactate, glycerol, and glucose. Cloned 16S rRNA gene sequences in contaminated sediment enrichments showed high sequence similarity to Gram-positive genera or to a single cultivated isolate from the Gram-negative, delta-*Proteobacterium*, *Anaeromyxobacter dehalogenans*. Sequences similar to *A. dehalogenans* were only detected under neutrophilic culture conditions. *Anaeromyxobacter* has recently been characterized as a facultative anaerobe using terminal electron acceptors such as Fe(III), nitrate (which is reduced to ammonia), fumarate, and chlorophenolic compounds for growth. All other organisms detected from the contaminated sediments were closely related to Gram-positive genera. Clone sequences obtained from the contaminated sediment enrichments cultured at low pH were all closely related to *Paenibacillus* and *Brevibacillus*. *Paenibacillus* has been found in the sediment and can reduce nitrate and utilize acetate as a carbon source. *Brevibacillus* has been found to utilize glucose as a carbon source, and is incapable of nitrate reduction. Both organisms also form

spores. However, no published studies are available on Fe(III) reduction by *Paenibacillus* and *Brevibacillus spp.* In neutrophilic enrichments from background sediments, the majority of culturable Fe(III)-reducers detected were closely related to the members of the *Geobacteraceae* family.

#### Groundwater “Bug Traps”

The effects of biostimulation on microbial biomass, community composition, and metabolic state have been monitored by deploying solid phase microbial samplers in wells at Area 1 prior to push-pull testing by Istok et al (Peacock et al. , 2004). Phospholipid fatty acid analysis and DGGE analysis of DNA was performed on extracts from the samplers. Viable biomass was higher in contaminated wells that received electron donor additions. DGGE profiles detected sequences related to genera capable of nitrate and Fe(III) reduction. Sequences affiliated with *Geobacter* were only detected in the wells that received electron donor additions, indicating that the additions stimulated the growth of metal-reducing organisms.

#### 4. HYDROLOGICAL, GEOCHEMICAL, AND MICROBIAL CHARACTERISTICS OF AREA 2

##### *Geology and Hydrology*

Area 2 is located several hundred feet to the southwest of the Ponds (Fig. 15). Most contaminants detected at Area 2 were probably transported to Area 2 through an historic stream channel of Bear Creek during operation of the Ponds. Because of this, the entire substance domain between Area 3 and Area 2 is most likely contaminated. A typical geologic profile at Area 2 would consist of about 6 meters of reworked fill and saprolite at the surface underlain by 2 meters of intact saprolite with weathered bedrock below the saprolite. The reworked fill tends to have a higher hydraulic conductivity than the native saprolite. Based on data from a tracer study test conducted in 1998 (Watson et. al. 1998) the rate of interstitial groundwater movement in the unconsolidated fill was calculated to range from 0.7 m/day to 4.5 m/day, with an average rate of about 2.2 m/day. Hydraulic monitoring at the site indicates that the depth to groundwater is approximately 4.5 meters from the surface and the hydraulic gradient ranges between about 0.01 and 0.025 to the southwest towards the Creek. Vertical upward gradients between the shale bedrock and unconsolidated zone are as great as 0.25.

##### *Geochemistry*

The Area 2 site is a shallow pathway for the migration of groundwater contaminated with uranium (12 mg/L) to seeps in the upper reach of Bear Creek (which is adjacent and both down-dip and down-strike to Area 2). Groundwater nitrate concentrations are generally lower (i.e., <100 mg/L) at Area 2 but have been detected above 1,000 mg/L in several of the wells. Groundwater technetium is generally detected below 600 pCi/L, and total dissolved solids concentrations (approximately 1,000 mg/L) are generally lower than Areas 1 and 3. The pH of groundwater at Area 2 tends to be between 6 and 7 with dissolved oxygen content about 1-2 mg/L. Areas of higher and lower uranium and nitrate exist at Area 2. For example TPB-16 which is representative of an area with higher uranium and lower nitrate contains 28 mg/L nitrate, 98 mg/L sulfate, 310 mg/L chloride, 60 mg/L inorganic carbon, 2 mg/L organic carbon, and 1.3 mg/L uranium. In contrast, well FW003, which is representative of an area with higher nitrate and lower uranium contains 1059 mg/L nitrate, 16 mg/L sulfate, 183 mg/L chloride, 89 mg/L inorganic carbon, 13 mg/L organic carbon, and 0.01 mg/L uranium. As much as 300-500 mg/kg of uranium may be associated with the solid phase material

An 8-9 meter-deep trench bisects Area 2 in an east to west direction. The trench was filled with gravel except for an 18-meter-long section in the middle, which was filled with zero-valent iron. Guar gum slurry was added during excavation to prevent the trench walls from collapsing. The trench is oriented nearly parallel to the direction of groundwater flow and is designed to use both the natural groundwater gradient and the permeability contrast between the gravel and iron in the trench and the native silt and clay outside the trench to direct flow through the iron treatment zone (Gu, Watson, et. al., 2000).

##### *Microbiology*

Almost half of the 16S rRNA gene library from groundwater monitoring well TPB16 within Area 2 had less than 95% nucleotide identity with previously observed sequences, and at least nine

bacterial divisions were represented, including *Acidobacterium*, *Cytophagales*, *Nitrospira*, high G+C, low G+C,  $\alpha$ -,  $\beta$ -,  $\gamma$ -, and  $\delta$ -*Proteobacteria* (Table 3). The  $\beta$ -*Proteobacteria* appeared to be a predominant sub-division, represented by *Azoarcus*, *Herbaspirillum*, *Zoogloea*, *Acidovorax*, *Achromatium*, and *Ralstonia*-like species (Fields et al., 2003). These results indicated that the microbial community from TPB-16 groundwater was extremely diverse. The TPB-16 site was the least contaminated compared to background, and had the most similar community structure with the background sample. Almost half of the 16S rRNA gene library from well FW-003 in Area 2 were affiliated with *Rhizobium* species, and the majority of these sequences had 99% nucleotide identity with an uncultured clone and *Rhizobium giardinii* (Table 3).

Table 3. Clonal libraries from the FRC contaminated areas

| Groundwater sample | Genera detected via SSU rRNA clonal libraries  |
|--------------------|--|
| FW-005 (Area 3)    | <i>Azoarcus</i> spp., <i>Ralstonia</i> spp., <i>Acidovorax</i> spp., <i>Delftia</i> spp., <i>Variovorax</i> spp., <i>Leptothrix</i> spp., <i>Aquaspirillum</i> spp., <i>Burkholderia</i> spp., <i>Pseudomonas</i> spp.   |
| FW-010 (Area 3)    | <i>Azoarcus</i> spp., <i>Ralstonia</i> spp., <i>Acidovorax</i> spp., <i>Delftia</i> spp., <i>Variovorax</i> spp., <i>Leptothrix</i> spp., <i>Aquaspirillum</i> spp., <i>Burkholderia</i> spp., <i>Pseudomonas</i> spp.   |
| TPB-16 (Area 2)    | <i>Nitrospira</i> spp., <i>Cytophaga</i> spp., <i>Acidobacterium</i> spp., <i>Chlorobium</i> spp., <i>Polyangium</i> spp., <i>Azoarcus</i> spp., <i>Zoogloea</i> spp., <i>Acidovorax</i> spp., <i>Ralstonia</i> spp., <i>Hyphomicrobium</i> spp., <i>Methylobacter</i> spp., <i>Pseudomonas</i> spp. |
| FW-003 (Area 2)    | <i>Pseudomonas</i> spp., <i>Rhizobium</i> spp., <i>Azoarcus</i> spp., <i>Nitrospira</i> spp., <i>Acidovorax</i> spp., <i>Rubrivivax</i> spp., <i>Herbaspirillum</i> spp.   |

Matthew W. Fields, Tingfen Yan, Sung-Keun Rhee, Susan L. Carroll, and Jizhong Zhou

- The microbial community composition at contaminated sites was altered compared to background, and the contaminated sites displayed decreased diversity
- All sites contained *Acidovorax* and *Pseudomonas* species, but at different relative abundances
- The acidic sites (FW-005, FW-010, and FW-015) were predominated by *Azoarcus* and *Pseudomonas* (approximately 70% of the respective libraries)
- Principal components analysis indicated that the sites were not similar with respect to community composition and distribution, and sites FW-015 and FW-010 were the only sites that were grouped
- The high nitrate sites were predominated by OTUs closely related to known denitrifiers (*Azoarcus*, *Acidovorax*, *Ralstonia*, *Pseudomonas*, *Zoogloea*)

*Azoarcus* comprised 17% of the library, *Pseudomonas* comprised 6%, and *Acidovorax* comprised almost 5%. Interestingly, *Acidovorax* species were a predominant group that was isolated from

FW-003 with enrichment cultures. These results indicated that the microbial community structure and composition were different from the other high nitrate sites, but FW-003 had circum neutral pH levels. *Chromobacterium* species predominated the obtained isolates from TPB-16, and these isolates had approximately 96% nucleotide identity with the  $\beta$ -*Proteobacterium*, *Chromobacterium violaceum* (Table 3). A different cluster of  $\beta$ -*Proteobacteria* isolates had 99% identity with *Janthinobacterium lividum*, and 96% identity with *Duganella* and *Zoogloea*. The Pseudomonad isolates resembled *Pseudomonas kilonensis*, *fragi*, and *veronii* and had between 97% and 99% identity. Isolate M-33 had 91% identity with *Clostridium acidisoli*, and five isolates had 94 to 98% identity with *Microbacterium oxydans*. The majority of bacterial isolates from the were  $\beta$ - and  $\gamma$ -*Proteobacteria*, and *Acidovorax* species predominated. The  $\gamma$ -*Proteobacteria* appeared to be closely related to known nitrate-reducers such as *Enterobacter*, *Klebsiella*, and *Acinetobacter* as well as the denitrifier, *Pseudomonas*. All  $\beta$ -*Proteobacteria* isolates from FW-003 were *Acidovorax*- or *Delftia*-like isolates. The Gram-positive isolates were not closely related (<93%) to previously observed sequences, and the closest relatives appeared to be *Sporomusa* and *Anaerovibrio* species. One isolate appeared to be classified in the *Cytophagales* division as a *Flavobacterium*. Modified FW-026 groundwater was inoculated with a mixture (1:1:1:1) of four isolates from site FW-003 or five isolates from TPB-16 and amended with different nutrients. Nitrate was reduced with the formation of nitrogen gas, and a significant concentration of nitrite was not observed (<2 ppm). The addition of trace minerals did not significantly increase the growth rate or the reduction of nitrate. These results indicated that selected isolates from FW-003 or TPB-16 could denitrify FW-026 groundwater once the pH and nitrate were adjusted. In addition, analyses of *nirS* gene fragments suggested that FW-003 and TPB-16 groundwater contained different, previously unobserved *nirS* genes that were not observed at the background, Area 1, or Area 3 samples.

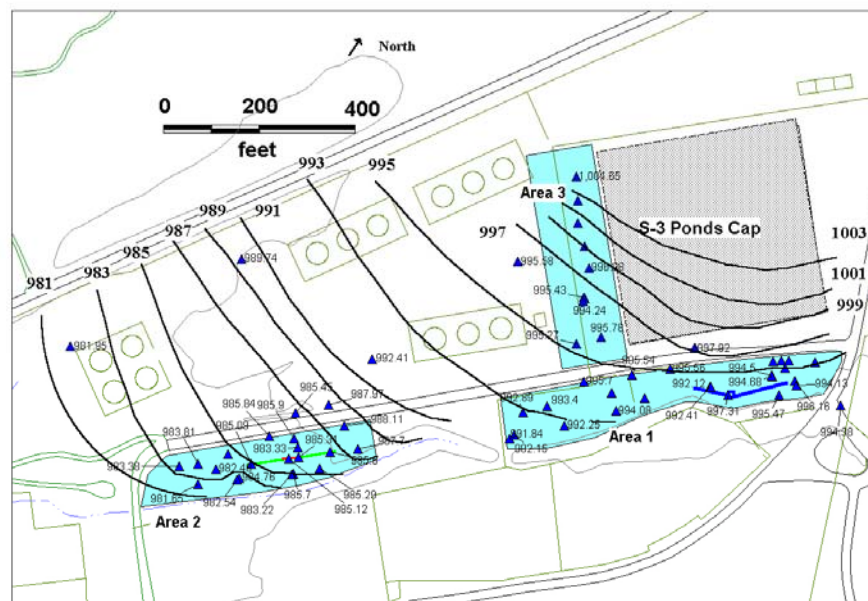
The reactive barriers at the S-3 Ponds site were installed using guar gum. After the guar was broken down by injecting an enzyme, microbial activity in the gravel filled trenches associated with the barriers increased dramatically particularly with sulfur and iron reducing microbes. Pre-guar gum concentrations of nitrate (>1,000 ppm) and uranium (>2 ppm) in these trenches were reduced dramatically to the low ppb level after the guar gum was injected, suggesting the potential for removal of these contaminants through microbial activity.



## 5. HYDROLOGICAL, GEOCHEMICAL, AND MICROBIAL CHARACTERISTICS OF AREA 3

### *Geology and Hydrology*

Area 3 is just west of the S-3 Ponds directly down strike (Fig. 15). A typical geologic profile at the Area 3 field plot would consist of about 1 meter of reworked fill and saprolite at the surface underlain by about 2 to 16 meters of intact saprolite with weathered shale bedrock below the saprolite. Based on geophysical studies conducted at Area 3 and observations made during the installation of monitoring wells, the thickness of saprolite in the southern portion of Area 3 is about 15.6 meters thick but only about 2 to 3 meters thick in the northern portion of the study area. Hydraulic conductivity of the shallow saprolite is fairly low ( $<0.26$  m/day) with maximum pumping rates of  $<1$  liter/minute. However, the permeability of the deeper saprolite (9 to 15.6 meters) in the southern portion of Area 3 is higher and can be pumped at rates of 5 liters/minute or more. Groundwater flux within this interval is estimated to be an average of 0.5 m/d based on point dilution measurements. This deep saprolite zone (e.g. 38 to 45 ft. ) is probably a preferential pathway for contaminants away from the S-3 Ponds. It is this zone where U concentrations are highest suggesting a high contaminant mass flux through this regime. Contaminant plumes appear to move preferentially along strike, which is the preferred direction of groundwater flow, and vertically downward as a result of density driven flow. Hydraulic monitoring indicates that the depth to groundwater is approximately 3.5 meters from the surface and the hydraulic gradient is fairly flat (Figure 16).



Several forced and natural gradient tracer studies have been conducted in Area 3 in an effort to quantify the influence of preferential flow and matrix diffusion on contaminant fate and transport. The tracer studies corroborated earlier findings that the transition zone directly above the bedrock is conducive to rapid preferential movement of solutes. Matrix diffusion into saprolite blocks is also an important mechanism governing solute fate and transport. Numerical simulation of observed tracer concentration breakthrough profiles suggested solute mass transfer rates were on the time-scale of months to years.

Geophysics was also used in Area 3 to identify probable areas of contaminant transport. Electrical resistivity contours and seismic velocity contours agreed well with direct borehole geochemical and hydrological measurements and provided an integrated, 3-dimensional view of the contaminant plume in Area 3. The geophysics results helped guide the placement of future wells and inspired their utility in defining a new area (Area 4) downgradient Area 3.

### *Geochemistry*

Due to its close proximity to the S-3 Ponds, contaminants (i.e., nitrate, technetium, uranium, volatile organic compounds such as PCE, and other common anions and cations) are detected at the greatest concentrations in both the groundwater and solid phase of Area 3 relative to Areas 1 and 2. The data tables for Area 3 are grouped into shallow saprolite wells, intermediate saprolite wells that are in the preferred flow path (e.g. FW024 and FW026), and deep bedrock wells (GW-243). Nitrate concentrations at the Area 3 field plot in groundwater are approximately 9,000 mg/l, uranium is as high as 60 mg/l, and technetium-99 is as high as 40,000 pCi/l. Peak concentrations of U in solution occur near the transition zone between 38 and 45 ft. This regime is a high discharge zone that has a measured bulk flux of 0.5 to 1.0 m/d. The north section of Area 3 has groundwater nitrate concentrations as high as 40,000 mg/L and very little U (e.g. <1.0 mg/L). The pH of groundwater at the Area 3 field plot tends to be more acidic than Area 2 (< 4.0) and it is highly buffered due to the high solute concentration in the groundwater. Thus, groundwater is an aggressive corrosive that has and continues to dissolve the soil solid phase at an accelerated weathering rate. Because of this, aqueous  $Al^{3+}$  concentrations can be as high as 700 mg/L. Since Al can readily hydrolyze and polymerize above pH 4.0, adjusting the groundwater pH upward causes Al floc formation and the co-precipitation of groundwater metals. The dissolved oxygen content of the groundwater is about 1-2 mg/L and sulfate concentrations can be as high as 2,000 mg/l. Calcium, sodium, magnesium, and manganese are other metals detected at significant concentrations (>100 mg/l) at the site. Tetrachloroethylene (3.3 mg/l), acetone (0.7 mg/l), and some other volatile organic compounds (VOCs) are also detected at the Area 3 field plot.

U-233/234 was detected at a maximum concentration of 17 pCi/g and average concentration of 2.1 pCi/g. U-238 was detected at a maximum concentration of 43 pCi/g and average concentration of 4.6 pCi/g. Concentrations of metals and radionuclides were highest near the southwest corner of the former S-3 Ponds. This is the primary area targeted for in situ sampling and research. An additional

10 borings were drilled and sampled for a technology demonstration project in the residuum southwest of the S-3 Ponds. The samples were analyzed for uranium only. The maximum concentration of U-238 detected in these samples was 162 pCi/g (490 ppm). All of the samples from the residuum are depleted relative to the amount of U-235 present (i.e., U-235/U-238 is <4.6%). There appears to be zones of elevated uranium in the unsaturated zone at a depth of 2 to 3 ft near the water table at a depth of 8 to 10 ft, and near the middle of the residuum at a depth of 19 to 20 ft (Fig. 17). Additional core samples acquired to a depth of bedrock (50ft) suggested the highest U solid phase concentrations were near the transition zone at a depth of 38 to 45 ft, where upwards of 750 mg/kg U were found on the sediments. Below 45 ft., solid phase U concentrations dropped well below 50 mg/kg due to the increasing presence of carbonate bearing minerals and pH regimes above 6.5 (Fig. 18).

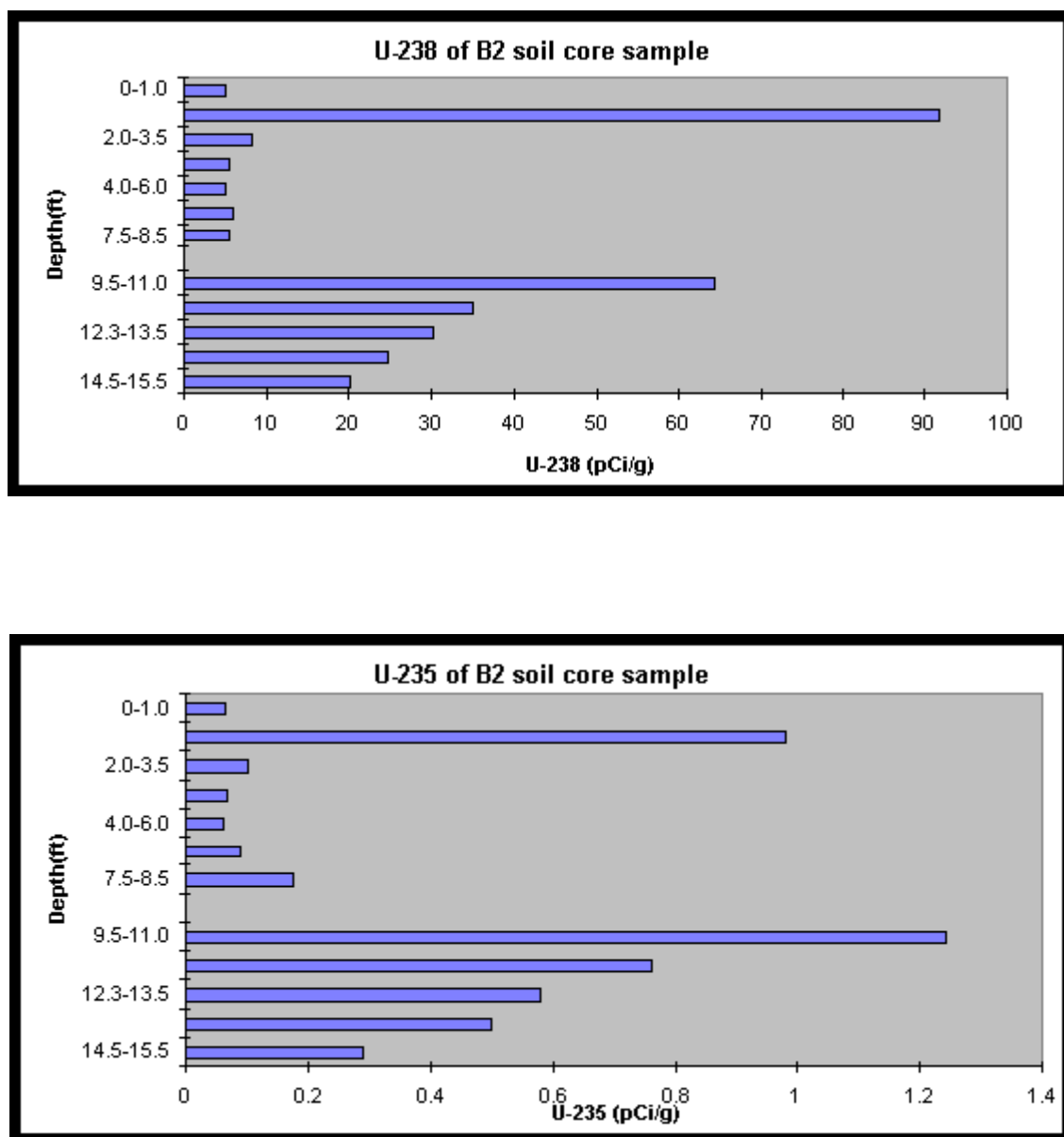


Figure 17. Solid phase U-235 and U238 concentration with depth near the S-3 Ponds.

The concentration of uranium in the Nolichucky Shale and Maynardville Limestone bedrock has not been characterized. The concentrations of uranium in the Maynardville Limestone are likely to be low or not detectable because the concentrations in groundwater are relatively low ( $< 0.30$  ppm) since the Maynardville is not directly below a source area. However, the concentration in the shallow Nolichucky shale in the vicinity of the S-3 Ponds may be higher because concentrations of uranium in groundwater have historically been detected at concentrations as high as 44 ppm with an average of 2.9 ppm.

Solid phase U concentrations in the 38 to 45 ft. preferred flow zone are as high as 750 mg/kg (Fig. 18). X-ray Absorption Spectroscopy (XAS) suggest that the U is complexed with solid phase P and possibly carbonates (Kemner et al., 2003, unpublished data, ANL). These results agree with SEM-EDX analyses of the solid phase that suggest U is highly correlated with P and Fe. Thus, U-P complexes are most likely associated with Fe-oxides that coat the solid phase minerals in these soils. These results agree with the findings of Bostick et al. (2002) and Barnett et al. (2000, 2002).

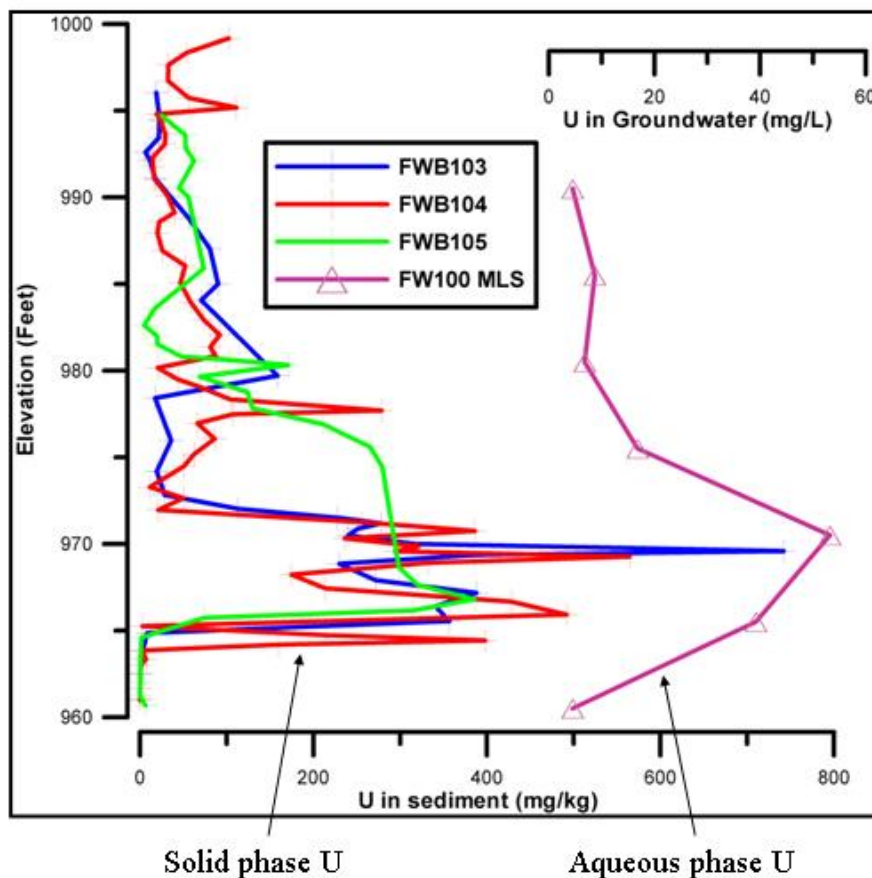


Figure 18. Solid phase uranium distribution on core material from Area 3 overlain with groundwater uranium concentrations acquired from the same depth. Elevated uranium concentrations at the 965 to 970 elevation depths are consistent with a known preferential groundwater conduit that exist at this depth.

## Microbiology

### Sediments

Subsurface sediments from the wells FWB-107 (13.2 m) and FWB-109 (15.4 m) in Area 3 were serially diluted in a basal salts medium (NaCl, NaHCO<sub>3</sub>, NH<sub>4</sub>Cl, minerals, 99/1% N<sub>2</sub>/CO<sub>2</sub>) with 5 mM lactate and 5 mM ethanol. The dilutions were provided with nitrate, Fe<sup>3+</sup>-citrate, or sulfate and incubated anaerobically at approximately 18 to 20°C. The results are summarized in Table 4 below:

Table 4. Area 3 incubations

|                  | <b>NO<sub>3</sub>-reduction</b> | <b>Fe<sup>3+</sup>-citrate reduction</b> | <b>SO<sub>4</sub> reduction</b> |
|------------------|---------------------------------|--|---------------------------------|
| FWB-107 (13.2 m) | 3500 cells/g                    | 46 cells/g                               | 240 cells/g                     |
| FWB-109 (15.4 m) | 5400 cells/g                    | 1700 cells/g                             | 1100 cells/g                    |

The nitrate tubes also displayed growth indicative of fungi in the higher dilutions, but only growth indicative of bacteria was scored. It also should be noted that the above samples were achieved from the auger tip at the bottom of the well (e.g., outside sediment was removed with sterile spatula, and intact sediment removed from the auger).

Studies by Lovley et al. 2003 focused on the subsurface sediments at Area 3 (FW 024; pH 4.1). Clone libraries of 16S rRNA gene sequences were generated. No sequences closely related to known metal- or sulfate-reducing bacteria were observed, before or after addition of electron donors to the sediment. A variety of enrichments was initiated from FW 024 sediment. Cultures were established at pH 4.5 and pH 7. Oxygen, nitrate, and U(VI)-reducers were enriched at low and high pH. Fe(III)-reducers were enriched with soluble Fe(III) at low and high pH. Microorganisms able to reduce Fe(III) oxides only grew at high pH. No growth was observed when enrichments were transferred to media without sediment. Neutrophilic U(VI)-reducing enrichments contained sequences closely related to *Geobacter*, *Geothrix*, *Desulfitobacterium*, and *Desulfosporosinus*. A pure culture, identified as *Salmonella bongorii*, was obtained that was capable of nitrate and U(VI) reduction (Lovley et al., 2003).

## Groundwater

Phylogenetic analysis of groundwater 16S rRNA clonal library has been conducted at the Area 3 site (Fields et al., 2003, Table 3).  $\beta$ -*Proteobacteria* appear to be a predominant sub-division (60% of library), represented by *Azoarcus*, *Zoogloea*, *Acidovorax*, and *Ralstonia*-like species. Nitrate-reducing microorganisms have been isolated, and are able to denitrify amended groundwater from Area 3. Denitrifying FRC isolates (*Proteobacteria* and Gram-positive bacteria) were able to denitrify amended groundwater from field sites, and the addition of meta-phosphate but not trace minerals increased denitrification. Iron- and sulfate-reducing enrichments have been achieved, and both can effectively reduce uranium in an artificial groundwater medium. Reduction rates with sulfate-reducing cultures are on the time-scale of hours to days which is encouraging with regard to pending in situ biostimulation endeavors.

Nitrate-contaminated groundwater samples have also been analyzed for *nirK* and *nirS* gene diversity. The samples differed with respect to nitrate, uranium, heavy metals, organic carbon content, pH, and dissolved oxygen levels. A total of 958 *nirK* and 1162 *nirS* clones have been screened by RFLP analysis, and 48 and 143 unique *nirK* and *nirS* clones, respectively, were obtained. A single dominant *nirK* restriction pattern was observed for all six samples, and was 83% identical to the *Hyphomicrobium zavarzinii nirK* gene. A dominant *nirS* pattern was observed for four of the samples, including the background sample, and was 95% identical to the *nirS* of *Alcaligenes faecalis* (Table 3). Diversity indices for *nirK* and *nirS* sequences were not related to any single geochemical characteristic, but results suggested that the diversity of *nirK* genes was inversely proportional to the diversity of *nirS*. Principal component analysis of the sites based on geochemistry grouped the samples by low, moderate, and high nitrate, but principal components analysis (PCA) of the unique operational taxonomic units (OTUs) distributions grouped the samples differently. Many of the sequences were not closely related to previously observed genes, and some phylogenetically related sequences were obtained from similar samples. The results indicated that the contaminated groundwater contained novel *nirK* and *nirS* sequences, functional diversity of both genes changed in relation to the contaminant gradient, but the *nirK* and *nirS* functional diversity was affected differently.

The estimated, cultivable bacterial numbers from Area 3 groundwater were approximately  $10^3$  cells/ml at pH 6.5, and approximately  $10^2$  cells/ml at pH 4.0, whereas bacterial numbers in Area 2 groundwater were estimated to be approximately  $10^7$  cells/ml (M.W. Fields, unpublished results with MR2A medium). The bacterial numbers in Area 2 groundwater were estimated to be approximately  $10^6$  cells/ml with acridine orange direct counts, and approximately  $10^5$  cells/ml in Area 3 groundwater (M.W. Fields and S.L. Carroll, unpublished results). The direct microscopic counts from circumneutral groundwater were similar to the numbers estimated with culture-based methods, but direct counts of acidic groundwater were 2 to 3 log higher than estimated with culture-based methods. The preliminary results suggested that viable bacterial load was decreased at contaminated groundwater samplings in Area 3. Albeit the differences could be explained by the presence of dead cells, the higher numbers observed with the direct count method might represent as-yet uncultivated microorganisms at acidic, contaminated FRC sites.

### Groundwater Coupons

Studies by Geesey et al. 2003, involved deployment of “biofilm coupons” in some Area 3 groundwater wells. These were sterile, mineral particles suspended in a well, allowing a biofilm to colonize. Hematite coupons were used in initial experiments at wells of the background and Area 3 sites. Coupons were incubated in the wells for 8 weeks. Clone libraries of 16S rRNA gene sequences were generated for each coupon. Microbial communities associated with Area 3 were observed to be less diverse (containing about one-half the phylotypes) as those of the background site. Retrieved clone sequences were mostly associated with the beta and gamma Proteobacteria. Sequences most closely related to *Aquaspirillum* and *Alcaligenes* were predominantly detected in the background and Area 3 libraries, respectively. “Quick dip” control deployments of hematite coupons revealed that most clone sequences were associated with biofilm-forming organisms.

## 6. HYDROLOGICAL, GEOCHEMICAL, AND MICROBIAL CHARACTERISTICS OF AREAS 4 AND 5

These new field research sites are located along the primary groundwater contaminant flow paths to the east and west of the former S-3 Ponds. Note, in the figure below, that Area 4 also is west of Area 3, site of the Stanford-ORNL uranium reduction field project (Fig. 19). These sites are within a known geochemical groundwater and sediment gradient (e.g., pH increases and nitrate decreases) as the plume moves away from the source area—the S-3 Ponds. The first phase of site characterization (Geoprobe work conducting electrical conductivity logging and well installation, groundwater sampling and analysis, surface geophysics including resistivity and seismic tomography, and water levels) has been completed. A total of 16 new wells were installed, 8 each in Areas 4 and 5. Uranium was detected in Area 4 at concentrations as high as 28 mg/l and in Area 5 up to 44 mg/L. Nitrate was detected in Area 4 at concentrations up to 25,000 mg/L and in Area 5 at concentrations up to 6,100 mg/L. Phase 2 coring, well installation, sampling and analysis, pumping tests, and tracer tests started in July to help identify and characterize new field plots within the S-3 Ponds plume. Researchers interested in obtaining samples from, or conducting fieldwork at Areas 4 and 5 should contact Dave Watson ([watsondb@ornl.gov](mailto:watsondb@ornl.gov)). For more information, see the [FRC Site Characterization Plan Addendum](#).]

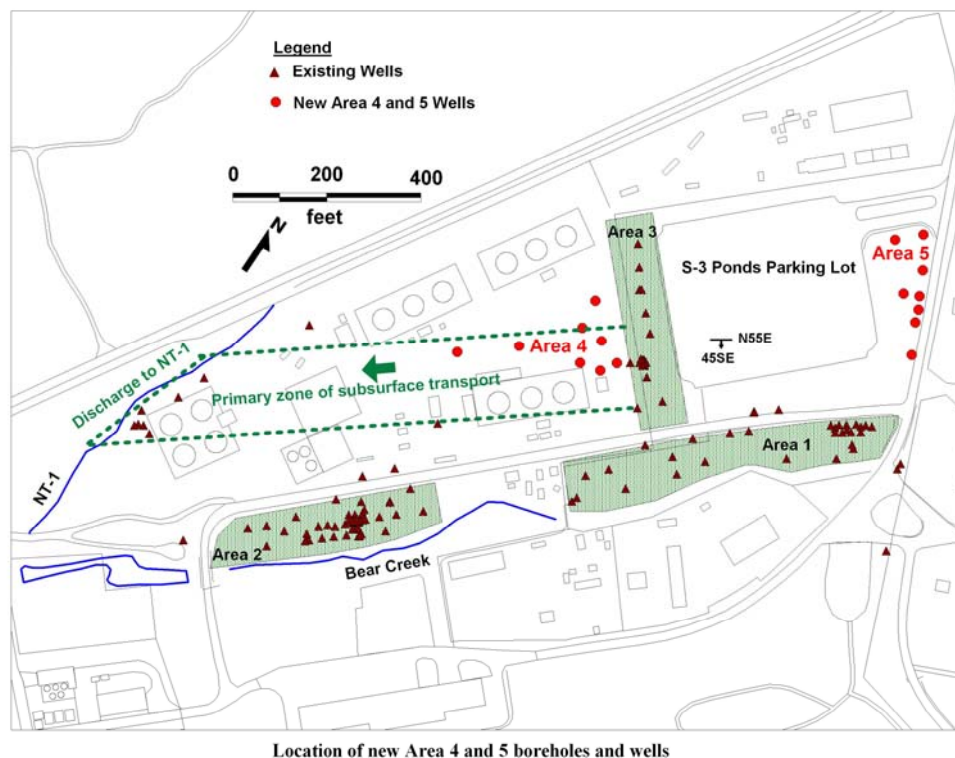


Figure 19. Location of new research areas 4 and 5.



## **7. RESEARCH NEEDS AT THE OAK RIDGE FIELD RESEARCH CENTER**

Potential research needs at the Oak Ridge Field Research Center:

### **1. General Microbiological Research Needs Across all the Contaminated Sites**

- Large-scale, concerted, analogous microbial characterization of FRC sites with different geochemical and geophysical attributes is needed for a more comprehensive understanding of site dynamics.
- In situ measurements for desired activities (nitrate-, sulfate-, metal-, and uranium-reduction) performed in conjunction with culture- and molecular-based characterization.
- Technology for real-time, in situ assessment of microbial communities and microbial activities during stimulations and/or augmentations.
- Study responses of microbial communities to stress and perturbations similar to FRC field conditions, and identify relevant microorganisms, activities, and marker signatures.
- Assess the interactions between microbial biochemical capacity and interactions with sediments and/or minerals, as well as nutrient limitations.
- Novel methods to accelerate bioreduction rates under acidic conditions.
- Develop methods to elucidate “active” members of populations during biostimulation.

### **2. General Hydrological Research Needs Across all the Contaminated Sites**

- Natural gradient multiple tracer studies to define rate and direction of groundwater movement and the magnitude of preferential flow and matrix diffusion.
- Large scale pump test to define well field interconnectedness.
- Studies are needed that quantify the rates and mechanisms of contaminant storage and release from the soil matrix porosity.
- Investigations that quantify the influence of large scale geologic heterogeneities (i.e. bedding planes, topography) on contaminant transport.
- Techniques are needed that overcome the diffusional barrier of the soil matrix that often limits remedial strategies in structured soils.

### 3. General Geochemical Research Needs Across all the Contaminated Sites

- Additional XANES, EXAFS, and Mossbauer investigations, before and after biostimulation, to define solid phase U species and chemical environment as well as Fe-oxide type. Speciation will dictate U bioreduction rate.
- Experiments that define the selectivity of U on the solid phase in the presence of competing cations, potential determining anions, and as a function of pH.
- Experiments addressing the intrusion of oxidants that may disrupt the stability of reduced U.
- Techniques that rapidly assess the spatial and temporal distribution of contaminants in both the aqueous and solid phase.
- Quantifying the rates and mechanisms of nanoparticle and colloid assisted contaminant transport .
- The influence of mineral oxide surface coatings on the geochemical behavior of contaminants.
- Noninvasive geophysical techniques are needed for plume mapping and defining preferential flow paths where contaminants reside.

### 4. General Numerical Research Needs Across all the Contaminated Sites

- Applications are needed for credible multiprocess, multipermeability, reactive transport models for simulating contaminant mobility in heterogeneous structured soils.
- High-performance contaminant transport simulators are needed for modeling contaminant mobility in hydrologically and geochemically complex media.
- Mechanistic numerical algorithms are needed that accurately describe contaminant mass transfer between preferential flow paths and the soil matrix.
- Network based visualization and modeling interfaces are needed for real-time visualization and steering of multiprocess numerical models on remote supercomputers.
- Model validation studies are needed that couple high-performance computing with multi-scale experimental datasets in structured soils.

## 8. REFERENCES

- Barnett, M.O., P.M. Jardine, S.C. Brooks, and H.M. Selim. 2000. Adsorption and transport of U(VI) in subsurface media. *Soil Sci. Soc. Am. J.* 64:908-917.
- Barnett, M.O., P.M. Jardine, and S.C. Brooks. 2002. U(VI) adsorption to heterogeneous subsurface media: Application of a surface complexation model. *Environ. Sci. Technol.* 36:937-942.
- Bostick, B.C., M.O. Barnett, P.M. Jardine, S.C. Brooks, S.E. Fendorf. 2002. Uranyl surface species formed on subsurface media from DOE facilities. *Soil Sci. Soc. Am. J.* 66:99-108.
- Cook, P. G., D. K. Solomon, W. E. Sanford, E. Busenberg, L. N. Plummer, and R. J. Poreda. 1996. Inferring shallow groundwater flow in saprolite and fractured rock using environmental tracers. *Water Resources Research*, 32(6):1501-1509.
- Dorsch, J., T. J. Katsube, W. E. Sanford, B. E. Dugan, and L. M. Tourkow. 1996. Effective Porosity and Pore Throat Sizes of Conasauga Group Mudrock: Application, Test and Evaluation of Petrophysical Techniques. ORNL/GWPO-021. Oak Ridge National Laboratory, Oak Ridge, Tennessee.
- Dreier, R. B., T. O. Early, and H. L. King. 1993. *Results and Interpretation of Groundwater Data Obtained from Multiport-instrumented Coreholes (GW-131 through GW-135); Fiscal Years 1990 and 1991*, Y/TS-803, Martin Marietta Energy Systems, Inc., Y-12 Plant, Oak Ridge, Tennessee.
- Fields et al., 2003
- Finneran KT, Housewright ME, Lovley DR. 2002a. Multiple influences of nitrate on uranium solubility during bioremediation of uranium-contaminated subsurface sediments. *Environ. Microbiology*. 4 (9): 510-516.
- Finneran KT, Anderson RT, Nevin KP, Lovley DR. 2002b. Potential for Bioremediation of uranium-contaminated aquifers with microbial U(VI) reduction . *Soil and Sediment Contamination* 11 (3): 339-357.
- Geesey G, Neal A, Rosso K, Gorby Y, Little B. 2002. Iron mineral surface physicochemical properties influence accumulation and detachment of iron reducing bacteria. ABSTRACTS OF PAPERS OF THE AMERICAN CHEMICAL SOCIETY 223: U595-U595 029-GEOC Part 1, APR 7 2002.
- Gierke, W. G., W. B. Lozier, and R. Pearson. 1988. Task 2, Well Logging and Geohydrologic Testing, Site Characterization and Groundwater Flow Computer Model Application, Vol. 1 of 6. ORNL/Sub30X-SA706C, Oak Ridge National Laboratory, Oak Ridge, Tennessee.
- Goldstrand, 1995

Gwo, J.P., P.M. Jardine, G.V. Wilson, and G.T. Yeh. 1995. A multiple-pore-region concept to modeling mass transfer in subsurface media. *J Hydrol.* 164:217-237.

Gwo, J.P., P.M. Jardine, G.V. Wilson, and G.T. Yeh. 1996. Using a multiregion model to study the effects of advective and diffusive mass transfer on local physical nonequilibrium and solute mobility in a structured soil. *Water Resource. Res.* 32:561-570.

Gwo, J.P., R. O'Brien, and P.M. Jardine. 1998. Mass transfer in structured porous media: embedding mesoscale structure and microscale hydrodynamics in a two-region model. *J Hydrol.* 208:204-222.

Gu, B., D.B. Watson, D.H. Phillips, and L. Liang. 2002. Biogeochemical, mineralogical, and hydrological characteristics of an iron reactive barrier used for treatment of uranium and other contaminants. Book chapter in: *Groundwater Remediation of Trace Metals, Radionuclides, and Nutrients, with Permeable Reactive Barriers*. D.L. Naftz, S.J. Morrison, J.A. Davis, C.C. Fuller (eds). Academic Press. 2002. pp. 305-342.

Hatcher, R. D., P. J. Lemiszki, R. B. Dreier, R. H. Ketelle, R. R. Lee, D. A. Leitzke, W. M. McMaster, J. L. Foreman, and S. Y. Lee. 1992. *Status Report on the Geology of the Oak Ridge Reservation*, ORNL/TM-12074, Martin Marietta Energy Systems, Oak Ridge National Laboratory, Oak Ridge, Tennessee.

Hoos, A. B., and Z. C. Bailey. 1986 *Reconnaissance of Surficial Geology, Regolith Thickness, and Configuration of the Bedrock Surface in Bear Creek and Union Valleys, Near Oak Ridge, Tennessee*, USGS Water-Resources Investigations Report 86-4165.

Istok JD, Senko JM, Krumholz LR, Watson D, Bogle MA, Peacock A, Chang YJ, White DC. 2004 In situ bioreduction of technetium and uranium in a nitrate-contaminated aquifer. *Environ. Sci. Technol.* 38 (2): 468-475.

Jardine, P. M., G. V. Wilson, and R. J. Luxmoore. 1988. Modeling the transport of inorganic ions through undisturbed soil columns from two contrasting watersheds. *Soil Sci. Soc. Am. J.* 52:1252-1259.

Jardine, P. M., G. K. Jacobs, and G. V. Wilson. 1993a. Unsaturated transport processes in undisturbed heterogeneous porous media. I. Inorganic Contaminants. *Soil Sci. Soc. Am. J.* 57:945-953.

Jardine, P. M., G. K. Jacobs, and J. D. O'Dell. 1993b. Unsaturated transport processes in undisturbed heterogeneous porous media II. Co-Contaminants. *Soil Sci. Soc. Am. J.* 57:954-962.

Jardine, P.M., W.E. Sanford, J.P. Gwo, O.C. Reedy, D.S. Hicks, R.J. Riggs, and W.B. Bailey. 1999. Quantifying diffusive mass transfer in fractured shale bedrock. *Water Resource. Res.* 35:2015-2030.

- Jardine, P.M., S.E. Fendorf, M.A. Mayes, I.L. Larsen, S.C. Brooks, and W.B. Bailey. 1999. Fate and transport of hexavalent chromium in undisturbed heterogeneous soil. *Environ. Sci. Technol.* 33:2939-2944.
- Jardine, P.M., G.V. Wilson, R.J. Luxmoore, and J.P. Gwo. 2001. Conceptual Model of Vadose-Zone Transport in Fractured Weathered Shales. (In) *Conceptual Models of Flow and Transport in the Fractured Vadose Zone*. U.S. National Committee for Rock Mechanics. National Research Council. National Academy Press, Washington D.C. p. 87-114.
- Jardine, P.M., T.L. Mehlhorn, I.L. Larsen, W.B. Bailey, S.C. Brooks, Y. Roh, and J.P. Gwo. 2002. Influence of hydrological and geochemical processes on the transport of chelated-metals and chromate in fractured shale bedrock. *J. Contamin. Hydrol.* 55:137-159.
- Koch, E., L. Toran, G. Moline, and K. Firestone, 1999. Modeling effective fractures in a well-characterized intact core. American Geophysical Union, Spring Meeting, Boston, MA, May 31-June 4, 1999.
- Kooner, Z. S., P. M. Jardine, and S. Feldman. 1995. Competitive surface complexation reactions of  $\text{SO}_4^{2-}$  and natural organic carbon on soil. *J. Environ. Qual.* 24:656-662.
- Law Engineering. 1983. *Results of Groundwater Monitoring Studies*, Y/SUB/83-47936/1.
- Lee, S. Y., L. K. Hyder, and P. D. Alley. 1991. Microstructural and mineralogical characterization of selected shales in support of nuclear waste repository studies. In *Microstructure of Fine-Grained Sediments: From Mud to Shale*, ed. R. H. Bennett, W. R. Bryant, and M. H. Hulbert, p. 545-560. New York: Springer-Verlag.
- Lee, R. R., R. H. Ketelle, J. M. Bownds, and T. A. Rizk. 1992. Aquifer analysis and modeling in a fractured, heterogeneous medium. *Ground Water* 30(4):589-597.
- Lovely et al., 2003
- Luxmoore and Huff, 1989
- Mayes, M.A., P.M. Jardine, T.L. Mehlhorn, B.N. Bjornstad, J.L. Ladd, and J.M. Zachara. 2003. Hydrologic processes controlling the transport of contaminants in humid region structured soils and semi-arid laminated sediments. *J. Hydrol.* 275:141-161.
- Moline, G. R., M. E. Schreiber, and J. M. Bahr. 1998. Representative ground water monitoring in fractured porous systems. *ASCE Journal of Environmental Engineering* 124(6):530-538.
- Moline, G. R., R. Ketcham, and C. R. Knight. 1997. Fracture-matrix exchange processes and their relationship to fracture characteristics. *EOS, Trans. Am. Geophys. Union* 78(17):S138.

Mulholland, P.J., G.V. Wilson, and P.M. Jardine. 1990. Hydrogeochemical response of a forested watershed: Effects of preferential flow along shallow and deep pathways. *Water Resource. Res.* 26:3021-3036.

Peacock AD, Chang YJ, Istok JD, Krumholz L, Geyer R, Kinsall B, Watson D, Sublette KL, White DC. 2004. Utilization of microbial biofilms as monitors of bioremediation. *Microbial Ecology*. 47 (3): 284-292.

Reedy, O. C., P. M. Jardine, G. V. Wilson, and H. M. Selim. 1996. Quantifying diffusive mass transfer of non-reactive solutes in columns of fractured saprolite using flow interruption. *Soil Sci. Soc. Am. J.* 60:1376-1384.

Sanford, W. E., and D. K. Solomon. 1998. Site characterization and containment assessment with dissolved gases. *ASCE Journal of Environmental Engineering* 124(6):572-574.

Schreiber, M. E.. 1995. Spatial variability in groundwater chemistry in fractured rock: Nolichucky Shale, Oak Ridge, TN. Unpublished M. S. thesis, University of Wisconsin - Madison, Madison, WI, 248 p.

Schreiber, M. E., G. R. Moline, and J. M. Bahr. 1999. Using hydrochemical facies to delineate ground water flowpaths in fractured shale. *Ground Water Monitoring and Remediation* 19(1):95-109

Senko et al., 2002

Shevenell, L. A. 1994. *Analysis of Well Hydrographs in a Karst Aquifer: Estimates of Specific Yields and Continuum Transmissivities*, Y/TS-1263, Martin Marietta Energy Systems, Inc., Oak Ridge Y-12 Plant, Oak Ridge, Tennessee, November.

Shevenell, L. A., and J. J. Beauchamp. 1994. *Evaluation of Cavity Occurrence in the Maynardville Limestone and the Copper Ridge Dolomite at the Y-12 Plant Using Logistic and General Linear Models*, Y/TJ-1022, Martin Marietta Energy Systems, Inc., Y-12 Plant, Oak Ridge, Tennessee, November.

Shevenell, L. S., R. B. Dreier, and W. K. Jago. 1992. *Draft Summary of Fiscal Year 1991 and 1992 Construction, Hydrologic and Geologic Data Obtained from the Maynardville Limestone Exit Pathway Monitoring Program*, YTS-814, Martin Marietta Energy Systems, Inc., Environmental Management Department, Health, Safety, Environment, and Accountability Division, Oak Ridge Y-12 Plant, Oak Ridge, Tennessee.

Solomon, D. K., G. K. Moore, L. E. Toran, R. B. Dreier, and W. M. McMaster. 1992. *Status Report - A Hydrologic Framework for the Oak Ridge Reservation*, ORNL/TM-12026, Martin Marietta Energy Systems, Inc., Oak Ridge National Laboratory, Oak Ridge, Tennessee.

U. S. Department of Energy (DOE). 1997a. *Report on the Remedial Investigation of Bear Creek Valley at the Oak Ridge Y-12 Plant, Oak Ridge, Tennessee*, DOE/OR/01-1455/V1&D2, Oak Ridge, Tennessee.

Van der Hoven, S. J., G. R. Moline, and D. K. Solomon. 1997. Spatial and temporal variations in major ion chemistry, O-18, and CFC in groundwater from a fractured rock aquifer. EOS 78(17):S158.

Wielinga et al., 2000

Wilson, G. V., and R. J. Luxmoore. 1988. Infiltration, macroporosity, and mesoporosity distributions on two forested watersheds. Soil Sci. Soc. Am. J. 52:329-335.

Wilson, G. V., J. M. Alfonsi, and P. M. Jardine. 1989. Spatial variability of subsoil hydraulic properties of two forested watersheds. Soil Sci. Soc. Am. J. 53:679-685.

Wilson, G.V., P.M. Jardine, R.J. Luxmoore, and J.R Jones. 1990. Hydrology of a forested watershed during storm events. Geoderma. 46:119-138.

Wilson, G.V., P.M. Jardine, R.J. Luxmoore, L.W. Zelazny, D.A. Lietzke, and D.E. Todd. 1991. Hydrogeochemical processes controlling subsurface transport from an upper subcatchment of Walker Branch watershed during storm events: 1. Hydrologic transport processes. J. Hydrology. 123:297-316.

Wilson, G.V., P.M. Jardine, R.J. Luxmoore, L.W. Zelazny, D.E. Todd, and D.A. Lietzke. 1991. Hydrogeochemical processes controlling subsurface transport from an upper subcatchment of Walker Branch watershed during storm events: 2. Solute transport processes. J. Hydrology. 123:317-336.

Wilson, G. V., P. M. Jardine, and J. P. Gwo. 1992. Modeling the hydraulic properties of a multi-region soil. Soil Sci. Soc. Am. J. 56:1731-1737.

Wilson, G. V., P. M. Jardine, J. D. O'Dell, and M. Collineau. 1993. Field-scale transport from a buried line source in unsaturated soil. J. Hydrology 145:83-109.